Building and Environment 200 (2021) 107959

Contents lists available at ScienceDirect

Building and Environment

journal homepage: www.elsevier.com/locate/buildenv

# Analysis of climate change impact on the preservation of heritage elements in historic buildings with a deficient indoor microclimate in warm regions

David Bienvenido-Huertas *, Miguel León-Muñoz, Juan Jesús Martín-del-Río, Carlos Rubio-Bellido

*Department of Building Construction II, University of Seville, 41012 Seville, Spain*

ARTICLE INFO

*Keywords:*
Churches
Indoor microclimate
Climate change
Multilayer perceptrons
Preservation
Heritage elements

ABSTRACT

Heritage preservation presents uncertainties in the global warming context. Both predicting the performance of environmental variables within the built environment and assessing the preservation conditions of heritage elements are today something of a challenge. Based on current monitorings, this study uses artificial intelligence to predict environmental performance in future scenarios. In addition, heritage elements are assessed according to threshold preservation values. The Chapel of the University of Seville was chosen as case study, applying both the threshold values from UNI 10829 and the performance index (PI) to assess the indoor environmental conditions. A total of 9 environmental treatment zones were identified according to temperature and humidity. To estimate the variables, the multilayer perceptron (MLP) was monitored and applied considering the time series of A2 future scenarios in each decade of the 21st century. The current MLP performances were analysed, thus showing a progressive reduction of the PI inside the church: at the end of the century, PI values oscillated between 6.6 and 6.8% in wooden objects, and between 1.8 and 2.3% in paintings. The results also showed a progressive increase in the number of hours and distance with respect to the optimal preservation values in the zones with a greater temperature and relative humidity, with cooling and dehumidification being the most effective strategies. This study represents a progress towards the most appropriate heritage preservation strategies by using an extrapolated methodology considering the climate change effect.

## 1. Introduction

Cultural heritage, whether tangible or intangible, is a legacy from countries and inhabitants for future generations [1]. Tangible cultural heritage includes historic buildings [2] and their heritage elements (e.g., paintings or frescoes). These tangible elements are non-renewable resources [3]. Their preservation for future generations is therefore among the main challenges of the professionals of the sector [4,5].

These existing heritage elements inside historic buildings could be often affected by the indoor microclimate [6]. Thus, microclimate significantly influences the possible deterioration of heritage elements, mainly due to the oscillations of temperature and relative humidity [7]. In addition, each material requires different temperature and relative humidity conditions, so the many materials in the indoor space should be considered when controlling the microclimate. Heritage elements have been appropriately preserved in some types of historic buildings, such as churches, so their indoor microclimate is supposed to be acceptable. However, aspects such as the use of HVAC systems [8,9], occupancy [10,11] or the existing damages in the envelope [12] could change indoor microclimate conditions. Although HVAC systems could be an appropriate measure to improve the microclimate in historic buildings under inappropriate conditions, they are usually used for users' thermal comfort [13]. In this regard, Lucchi [14] detected that the operational patterns of HVAC systems focused on thermal comfort could be incompatible with the preservation thresholds of each material. In Spain, most churches use HVAC systems only to guarantee users' thermal comfort [15]. However, this does not prevent from using this type of measures for preservation. Moreover, EN 15759-1 considers the possibility of using heating systems both for thermal comfort and preservation.

In the last decade, many studies have been focused on analysing both the impact of the indoor microclimate on the preservation of heritage elements and the establishment of measures to preserve them. Among the studies based on a long monitoring is Bonacina et al. [16]. For 20

* Corresponding author.
*E-mail address:* Jbienvenido@us.es (D. Bienvenido-Huertas).

https://doi.org/10.1016/j.buildenv.2021.107959
Received 29 March 2021; Received in revised form 4 May 2021; Accepted 10 May 2021
Available online 24 May 2021
0360-1323/

years, these authors conducted a monitoring to assess the preservation state of several heritage elements in the Scrovegni Chapel in Italy. The results showed the aspects that HVAC systems should guarantee to maintain the indoor microclimate. Nevertheless, the time cost required to draw conclusions could make the implementation of the monitoring methodology in the whole heritage-built environment something of a challenge. This type of studies could be performed with shorter monitoring campaigns. Rubeis et al. [12] made a multiobjective analysis in a damaged church through a monitoring lasting 1 year. Afterwards, the building was thermally modelled to estimate the indoor microclimate in view of both the variation of the operational conditions or the use of HVAC systems. This simulation process was reproduced by other authors [17–19] to obtain the improvement achieved by modifying the building.

However, in-situ monitorings allow to know aspects of the indoor microclimate that could be limited in the simulation processes. Aspects such as the variation of the thermal gradient in height could be difficult to be obtained in simulation processes. Varas-Muriel and Fort [20] assessed the microclimate in the Lady of the Assumption Church (Spain) to analyse the effect of a radiant floor heating system in the preservation of indoor materials. The monitoring through balloons with probes allowed the thermal gradient to be characterized like with CFD analyses. A similar methodology was used by Aste et al. [21] to characterize the Duomo's indoor microclimate (the Cathedral of Milan) through balloons with probes. The results showed that the stratification of temperatures in height were lower than 0.5 °C, except in the zones close to the gaps, most influenced by outdoor conditions.

In addition, the possibilities that could be achieved by restoring the envelope have also been addressed. Cardinale et al. [22] analysed the indoor conditions of the Matera Cathedral (Italy) before and after its restoration (a radiant floor heating system was included). The results showed that the integrated incorporation of a heating system, together with the restoration of the rest of the building, obtained appropriate indoor microclimate conditions both for preservation and thermal comfort. Likewise, it is crucial to consider the expected impact of the operational pattern of the building due to the impact of its occupants. Camuffo et al. [23] analysed the variation of the indoor microclimate in the church of Rocca Pietore when religious celebrations took place. The use of heating systems in masses increased the temperature in the upper part of the church, thus emerging condensations in the cold walls and degrading heritage elements.

Other studies focused on both the establishment of new data analysis methodologies and the design of new monitoring processes of indoor microclimate: (i) Silva and Henriques [24] analysed San Cristobal Church, in Portugal, focusing on the limitations of EN 15757 by applying it climates that are not cold. Consequently, an application methodology of the standard was used in mild climates, such as those in the central zone in Portugal; (ii) Anaf and Schalm [25] monitored the indoor microclimate of a church in Belgium to assess the peak and drop hours existing in the temperature and relative humidity time series. The analysis by frequency ranges allowed the existing danger due to the fluctuations of the indoor microclimate to be defined; (iii) Basto et al. [26] developed a measurement instrument to measure both environmental variables and the width of the crack; and (iv) García-Diego and Zarzo [27] applied probes in the frescoes to measure the surface hygrothermal conditions.

Moreover, the studies by Spolnik et al. [28], Chatoutsidou et al. [29], and Bencs et al. [30] showed the influence of heating systems on the dispersion of outdoor pollutant particles, thus becoming a new factor to be considered in the preservation analysis. Likewise, Kalamees et al. [31] analysed the impact of the indoor microclimate in naturally ventilated churches in cold climates. The results showed a high mould formation risk in these churches.

Churches have been widely used as case studies; however, other types of case studies have also been analysed. Andretta et al. [32] analysed the results obtained from the monitorings made both in summer and winter in the Classense Library in Ravenna, Italy. The results showed that the indoor microclimate conditions were not appropriate in most rooms of the library to preserve old books. In another study focused on libraries, Diulio et al. [33] analysed the most influential parameters to preserve 11 libraries in La Plata (Argentina). The results showed that some factors significantly influence the preservation of indoor spaces, e.g., the adjacent area to other spaces and the insulation level. Palace complexes have also been analysed. Torres-González et al. [34] assessed, among other aspects, the hygrothermal conditions in the microclimate around the plasterwork of the upper frieze in the Toledanos Room, in the Real Alcazar of Seville. In addition, museums have been widely used as case studies: (i) Sciurpi et al. [35] assessed the microclimate of the exhibition halls in La Specola museum in Florence; these exhibition halls were affected by overheating problems. The use of solar control glasses improved the indoor microclimate conditions; and (ii) another similar study, García-Diego et al. [36], analysed the most appropriate sampling conditions to characterize the indoor microclimate in the Sorolla room in the Pio V museum in Valencia (Spain). The results showed that the hourly sampling implied to know the fulfilment of the preservation conditions set by various standards. In these cases, the use of a classification system of the microclimate [37], management [38,39], and remote control [40] allows preservation, thermal comfort, and energy efficiency to be balanced.

However, the possible climate change impact on cultural heritage has been scarcely studied, although the impact is estimated to be significant [41] due to aspects such as the temperature rise, the variability of rainfalls and humidity, and the emergence of phenomena [42]. This requires proper management of heritage buildings with the risk of climate change [43]. Some studies have analysed the possible climate change effects from the perspective of damages in the building envelope or structure. Sevieri et al. [44] assessed the risk of typhoons in the roofs of cultural heritage assets, whereas García-Sánchez et al. [45] and Ezcurra and Rivera-Collazo [46] assessed the impact of the sea level rise on heritage buildings located on the coast. Verticchio et al. [47] assessed the indoor microclimate of a painting located in both a museum and a dwelling in various periods in Valencia. The projections were considered in two specific years of the ENSEMBLES-A1B scenario. The results showed a greater chemical risk for the material in spring. Prieto et al. [48,49] analysed the climate change effect on heritage buildings located in cold climate zones in Chile. The analysis was based on determining the functional useful life of the building in relation to climate change using the fuzzy logic methodology developed in subsequent works [50]. The results showed that, in cold regions, climate change could improve the useful life of these buildings. However, in warm zones, climate change implies a greater impact. The studies conducted in other scopes related to the climate change impact on buildings have shown that the greatest influence of the outdoor climate modification takes place in warm zones [51,52]. The characteristics of the indoor microclimate in churches could be significantly different from those in cold zones [53]. Moreover, the indoor microclimate state of the building could be deficient in a current context and highly dependent of the outdoor climate. De Rubeis et al. [12] showed that damaged historic buildings or historic buildings with a deficient state are more exposed to outdoor climate variations. Thus, climate change could impact this type of buildings. The objective of this study was the analysis of the climate change impact on the preservation of heritage elements of historic buildings with a deficient indoor microclimate. Climate change impact is expected to be greater in warm climate zones, so a case study located in a warm climate zone (the south of Spain) was analysed. For this purpose, the study predicted the indoor microclimate using artificial intelligence models. This use is based on the potential of using statistical models to make future estimates of the indoor microclimate. Thus, this study offers a new approach to the indoor microclimate analysis by considering both the climate change impact on the indoor microclimate and the possibility of using artificial intelligence models. Likewise, a methodology to analyse the preservation threshold values of UNI 10829 based on both environmental treatment zones and the Euclidean distance is suggested,

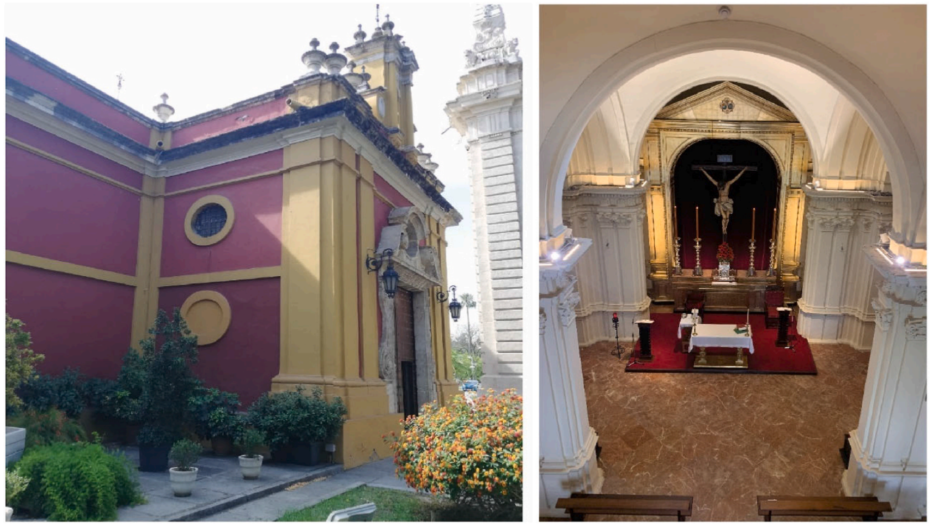

Fig. 1. Case study.

**Table 1**
Upper and lower limit values of temperature and relative humidity to appropriately preserve heritage elements according to UNI 10829.

| Artwork | Temperature [°C] | | Relative humidity [%] | |
|---|---|---|---|---|
| | Lower limit | Upper limit | Lower limit | Upper limit |
| Wooden objects | 19 | 24 | 50 | 60 |
| Paintings | 19 | 24 | 45 | 55 |

**Table 2**
Classification classes of the indoor microclimate according to the value of PI.

| Range of values | Class |
|---|---|
| PI $\geq$ 90 | A |
| 85 $\leq$ PI < 90 | B |
| 80 $\leq$ PI < 85 | C |
| PI < 80 | Not classified |

thus knowing the required air conditioning strategies. The key contributions of this document can be summarized as follows:

- Characterization of the climate change impact on the preservation of heritage elements in case studies with a deficient microclimate.
- Development of a methodology based on both environmental treatment zones and the Euclidean distance to determine environmental treatment strategies accurately.
- Study of the possibility of using artificial intelligence models to estimate the time series of the indoor microclimate. A methodology different from those based on energy simulation models could be established to characterize the microclimate in other scenarios.

## 2. Methodology

### 2.1. Case study

This study was aimed to assess the possible preservation risk in historic buildings with a deficient indoor microclimate in the current state. A case study located in a warm climate zone in the current scenario was selected due to the greater climate change impact expected in these regions [54,55].

The case study was the Chapel of the University of Seville (Fig. 1). The church was built between 1756 and 1763 in the complex of the old tobacco factory, which is today the headquarter of the University of Seville. The church has a floor plan in the shape of a Greek cross. The transepts are connected to the central nave through a rectangular door, and the latter is free of obstructions [56]. The façade is made of solid brick (with variable thickness in each orientation) and plaster cladding. The windows are monolithic glass. Regarding the operational pattern, ordinary services (masses) are held from Monday to Friday at 1:30 p.m. and 8:00 p.m., Saturdays at 8:00 p.m., and Sundays at 11:30 a.m. and 1:00 p.m. Likewise, tourists visit the building every day of the week.

Since 1966 there is a constant need for preservation actions in the heritage works of the building. One of the most important works inside the church is the sculpture of the Christ of the Good Death. This sculpture was restored in 1983, 1994, 2004, and 2018. These constant interventions are a sign that the heritage works inside the building are being quickly deteriorating. For this reason, environmental conditions could significantly influence their rapid degradation. In addition, this situation could have consequences because of the many historic and artistic heritage works inside the building.

Regarding the climate of Seville, the city is in the B4 climatic zone according to the classification of the Spanish Building Technical Code [57]. Thus, this area is characterized by mild winters, while summers correspond to the severest climatic typology in Spain. In summer, temperature values greater than 40 °C are obtained.

### 2.2. Assessment of the environmental conditions inside the church

The appropriate environmental conditions of the indoor microclimate in the church to preserve heritage elements were assessed with the threshold values from UNI 10829 [58]. For this purpose, the type of elements in the church were defined. The heritage elements inside the church can be divided into two types: wooden objects and paintings. Table 1 shows the threshold values of temperature and relative humidity to preserve these elements appropriately.

The analysis of the indoor environment quality level could be simplified by the performance index (PI) proposed by Corgnati et al. [59]. PI is the proportion of the number of monitored observations within the preservation limits (Eq. (1)). Thus, PI allows the quality level of the indoor microclimate to be quantified to preserve heritage elements. Likewise, the indoor environment quality could be classified by PI. Corgnati et al. [59] established four types. The three first correspond to PI values greater than 80% and are related to an appropriate indoor environment quality (Table 2). Thus, values lower than 80% could be related to an indoor microclimate that prevents from preserving heritage elements. PI values between 80 and 100% obtain various classification

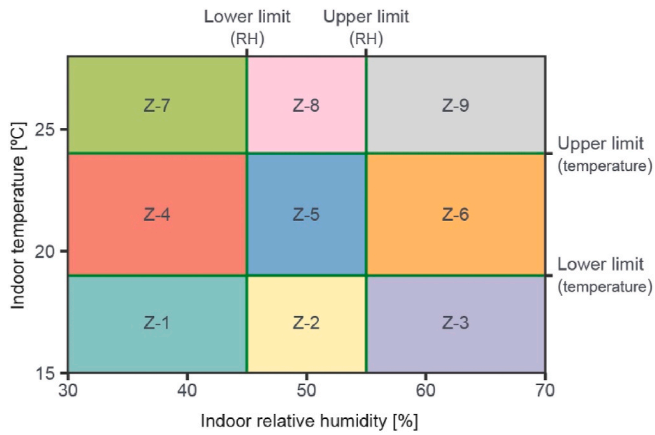


**Fig. 2.** Environmental treatment zones according to temperature and relative humidity.

levels. The criterion of using one class or another should be previously agreed by curators to establish design strategies [12,60]. Although this approach allows indoor climate to be quantified, some curators see complexity in the indicator as a time series of monitored or estimated data should be statistically analysed [5]. Nevertheless, many studies are based on the analysis of PI [12,33,60–62].

$$PI = 100\frac{n}{N} \tag{1}$$

Where $n$ is the number of observations between the upper and lower limits of temperature and relative humidity, and N is the total number of monitored observations.

The analysis of PI could be complemented with the variance indicator included in UNI 10829. The variance indicator is the ratio of observations outside the preservation thresholds. Although this type of approach is in line with UNI 10829 and PI, it could make the detailed analysis of the requirements of the indoor microclimate for an appropriate preservation something of a challenge. The reason is that it does not analyse if the problem presented by the indoor microclimate is based on low temperatures or on a high relative humidity. Thus, this study presents an analysis methodology based on 9 environmental treatment zones (Fig. 2). These zones are used based on the results obtained by Corgnati and Filippi [60] and by climate analysis tools such as Climate Consultant [63]. These zones allow the requirements for the indoor microclimate to be known, so correction strategies could be considered. Table 3 describes all these zones. Z-5 corresponds to the zone that fulfils the threshold values established by UNI 10829 for each material. Moreover, the percentage of observations in each zone could be determined. However, this aspect could not reflect the impact of environmental conditions on the appropriate preservation of heritage elements. For this reason, the distance of each observation is determined to the closest preservation point. In addition, a quantification is carried out through the Euclidean distance. Table 3 shows the Euclidean distances used in each zone, varying according to the closest preservation point. In Z-1, the closest preservation point corresponds to the coordinate of the lower values of both temperature and relative humidity established in UNI 10829, and in Z-9 are the upper values established in UNI 10829.

### 2.3. Estimating environmental variables

The indoor microclimate of the church was analysed in both the current and future scenario. The monitoring of the indoor microclimate was combined with the estimate of the hourly values of the various scenarios through artificial neural networks (Fig. 3). Artificial neural networks are a statistical model hardly developed by heritage studies [64,65] but used by environmental characterization studies [66,67].

**Table 3**
Descriptions of the environmental treatment zones according to temperature and relative humidity.

| Treatment zones | Comment | Equation [(i)] | |
|---|---|---|---|
| Z-1 | Zone with the environmental temperature and the relative humidity below the lower limits. | $d_i = \sqrt{(T_{low,limit} - T_i)^2 + (RH_{low,limit} - RH_i)^2}$ | (2) |
| Z-2 | Zone with the relative humidity between the limits established, but with the environmental temperature below the lower limit | $d_i = \lvert T_{low,limit} - T_i \rvert$ | (3) |
| Z-3 | Zone with the environmental temperature below the lower limit, and the relative humidity over the upper limit | $d_i = \sqrt{(T_{low,limit} - T_i)^2 + (RH_{up,limit} - RH_i)^2}$ | (4) |
| Z-4 | Zone with the environmental temperature between the limits established, but with the relative humidity below the lower limit | $d_i = \lvert RH_{low,limit} - RH_i \rvert$ | (5) |
| Z-5 | Zone within the preservation limits established by UNI 10829 | | |
| Z-6 | Zone with the environmental temperature between the limits established, but with the relative humidity over the upper limit | $d_i = \lvert RH_{up,limit} - RH_i \rvert$ | (6) |
| Z-7 | Zone with the environmental temperature over the upper limit, and the relative humidity below the lower limit | $d_i = \sqrt{(T_{up,limit} - T_i)^2 + (RH_{low,limit} - RH_i)^2}$ | (7) |
| Z-8 | Zone with the relative humidity between the limits established, but with the environmental temperature over the upper limit | $d_i = \lvert T_{up,limit} - T_i \rvert$ | (8) |
| Z-9 | Zone with the environmental temperature and the relative humidity over the upper limits | $d_i = \sqrt{(T_{up,limit} - T_i)^2 + (RH_{up,limit} - RH_i)^2}$ | (9) |

[(i)] $T_i$ and $RH_i$ are the value of indoor temperature and relative humidity in the observation $i$.

Artificial neural networks are made up of neurons that constitute data processing units. The artificial neural network can give an output value by processing the input information it receives. These models are used to solve linear and nonlinear problems [68,69]. Thus, complex problems are addressed, both classification [70,71] and regression [72–74]. Multilayer perceptrons (MLPs) are a type of artificial neural networks.

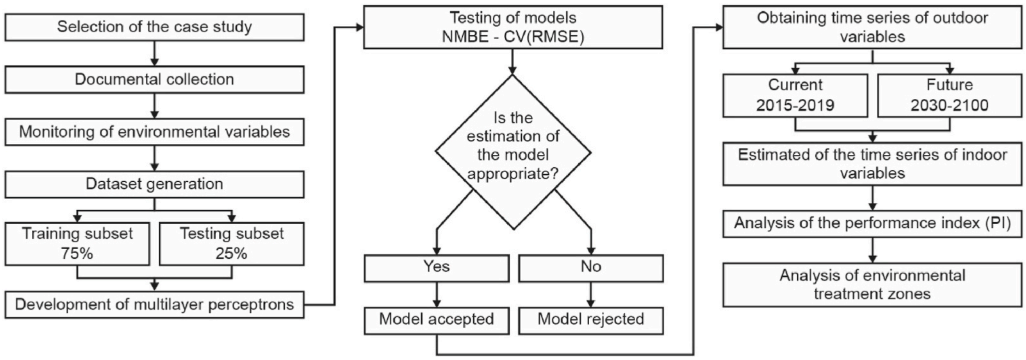


**Fig. 3.** Flowchart with the steps followed in the research.

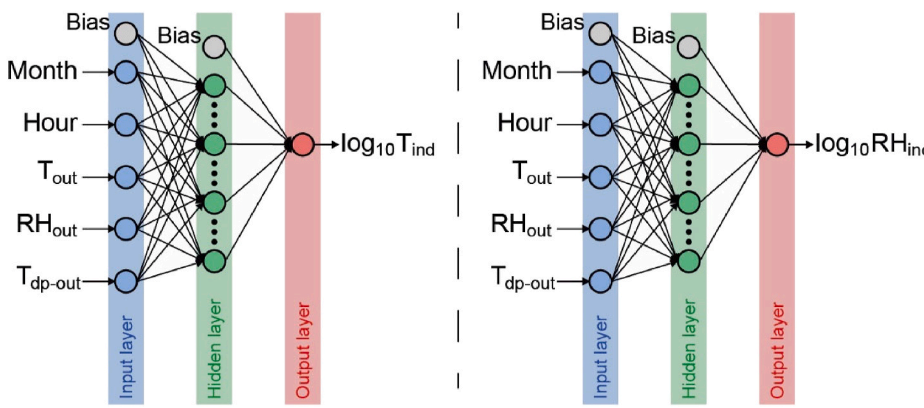


**Fig. 4.** Basic scheme of the MLPs designed.

**Table 4**
Input and output variables considered in the MLPs.

| Input variables | Output variables |
|---|---|
| Month, hour, $T_{out}$, $RH_{out}$, $T_{dp-out}$ | $\log_{10} T_{ind}$; $\log_{10} RH_{ind}$ |

MLPs are among the models obtaining the best results because of their universal approximation capacity [75–77]. One of the most important aspect is their architecture. In general terms, the architecture of MLPs is usually divided into three layers (Fig. 4): (i) an input layer, (ii) one or several intermediate layers, and (iii) and output layer. Each layer has a series of neurons interconnected with those in the following layer. The neurons of the input layer correspond to the input variables, and the neuron of the output layer correspond to the class or attribute to be estimated. The output value of each neuron is obtained by both adding the values of the input neurons weighted with synaptic weights and applying an activation function (Eq. (10)). These connections are propagated to the output layer (Eq. (11)), thus obtaining the value estimated by the multilayer perceptron ($\widehat{Y}_{MLP}$). This study used a sigmoidal activation function (Eq. (12)) in the whole architecture of the MLPs. The advantage of this type of function is that it compresses an infinite input set into a finite output set.

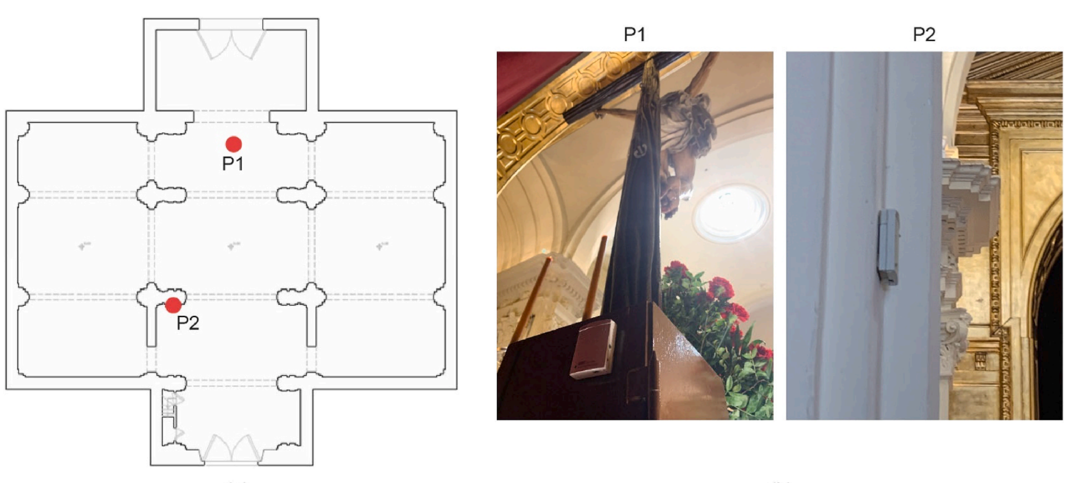


**Fig. 5.** Measurement points.

**Table 5**
Technical specifications of the equipment used.

| Equipment/ Probe | Variable | Measurement range | Accuracy | Limit value of EN 15758 and EN 16242 |
|---|---|---|---|---|
| HOBO U12-012 | Temperature | From −20 to +70 °C | ±0.35 °C | ±0.5 °C |
| | Relative humidity | From 5 to 95% | ±2.5% | ±2.5% |
| VAISALA HMP45D | Temperature | From −20 to +60 °C | ±0.2 °C | ±0.5 °C |
| | Relative humidity | From 0.8 to 100% | ±1% | ±2.5% |

$$y_k = \sigma\left(\sum_{j=1}^{d} w_{kj}^{(1)} x_j + w_{k0}^{(1)} x_0\right) \tag{10}$$

$$\widehat{Y}_{MLP} = \sigma\left(\sum_{k=1}^{M} w_{lk}^{(2)} \sigma\left(\sum_{j=0}^{d} w_{kj}^{(1)} x_j\right) + w_{l0}^{(2)} y_0\right) \tag{11}$$

$$\sigma = \frac{1}{1+e^{-x}} \tag{12}$$

Where $x_j$ are the input values, $w_{k0}^{(1)}$ and $x_0$ are the weight and the value of the bias neuron in the input layer, $w_{l0}^{(2)}$ and $y_0$ are the weight and the input value of the bias neuron in the hidden layer, $w_{kj}^{(1)}$ are the weights of the hidden layer, $w_{lk}^{(2)}$ are the weights of the output layer, $y_k$ is the output value of a neuron in the hidden layer, and $\sigma$ is the activation function.

The estimate given by the multilayer perceptron depends on the values of the synaptic weights. Therefore, the main objective of the algorithm is to select the value of the weights to reduce the error of the estimates. For this purpose, a learning algorithm is applied to a training dataset. In this study, the multilayer perceptrons were trained by backpropagation [78]. This type of learning first selects a random assignment of values to the synaptic weights, then a series of data is randomly included, and finally the error obtained between the output value of the model and the actual output value is analysed. The values of the synaptic weights are adjusted, and the process is repeated with the different instances of the dataset until the end of the process.

In the training of the multilayer perceptron, the appropriate training algorithm that minimizes the error function associated with the model should be selected. The Broyden-Fletcher-Goldfarb-Shanno (BFGS) [79] algorithm was used in this research work. This type of method has a significant advantage over Newton's method because they are faster and consume less resources by not requiring the direct calculation of the Hessian and its inverse. For this purpose, approximations of the inverse of the Hessian are calculated at each iteration.

The goal of these models was to estimate the hourly values of temperature and relative humidity inside the church in the scenarios considered. Thus, models with an input structure composed of outdoor climate variables which could be easily obtained were considered. Table 4 shows the input and output variables considered in the MLPs. The input variables were variables that could be obtained from the monitoring of the outdoor climate or from the obtaining of prediction time series of the climate in a region: outdoor temperature ($T_{out}$), outdoor relative humidity ($RH_{out}$), and outdoor dew temperature ($T_{dp-out}$). The use of outdoor climate variables could be an interesting option to

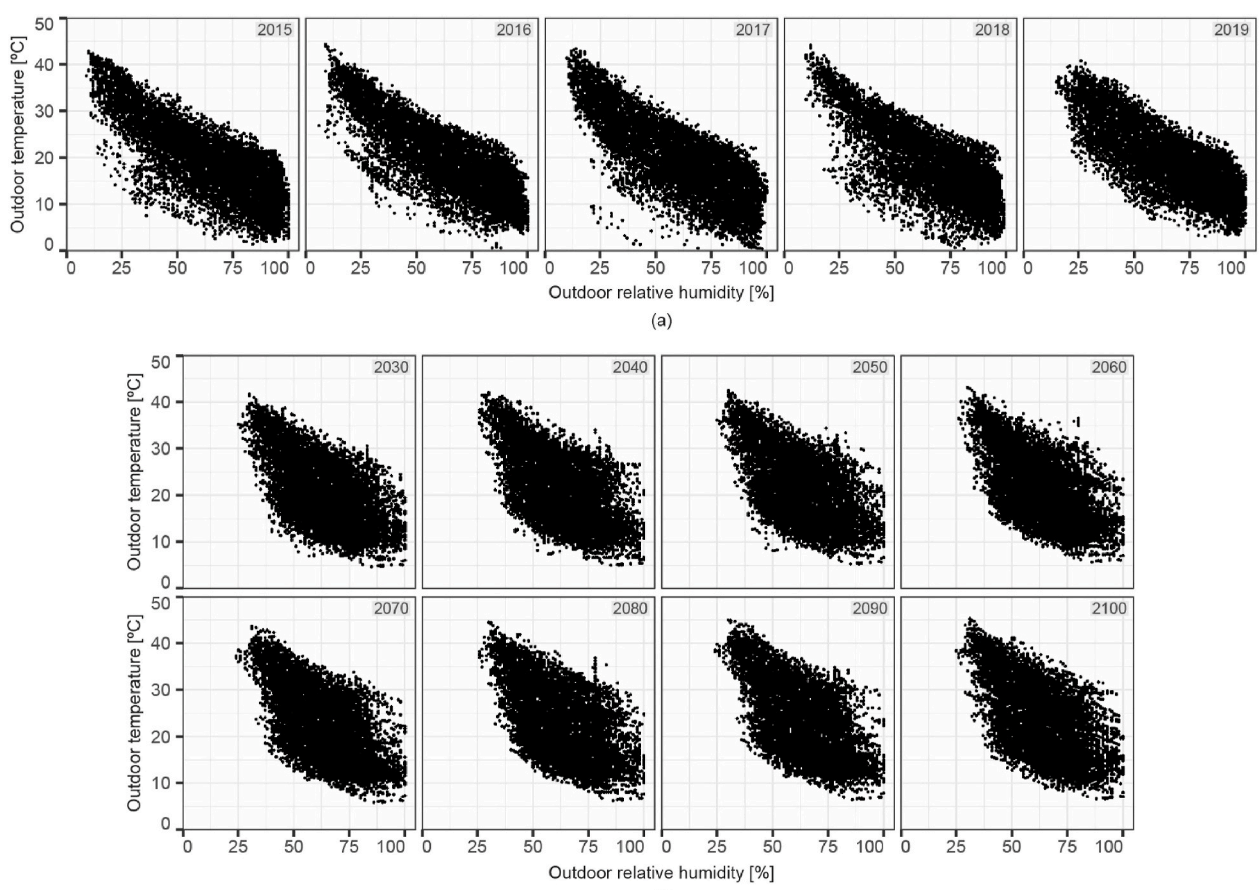


**Fig. 6.** Point clouds of the hourly outdoor temperature and relative humidity values obtained from the outdoor climate. The 2015–2019 values were measured with VAISALA HMP45D, and the 2030–2100 values were obtained with METEONORM.

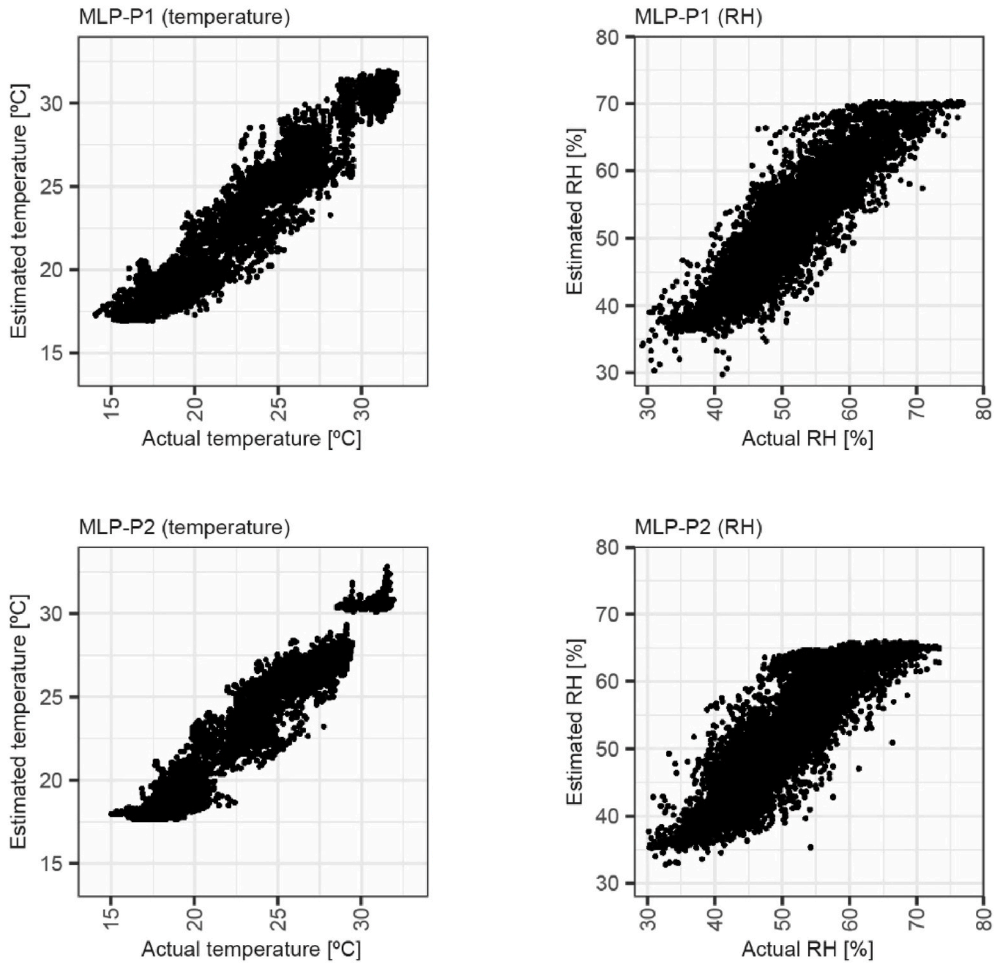


**Fig. 7.** Point clouds between the actual and the estimated value in the time serie monitored.

**Table 6**
Performance of the estimate obtained, and comparison with the limit values from ASHRAE Guideline 14.

| Point | Variable | NMBE [%] | | CVRMSE [%] | |
|---|---|---|---|---|---|
| | | Value obtained | Limit value | Value obtained | Limit value |
| P1 | Indoor temperature | −1.03 | ±10 | 5.43 | 30 |
| | Indoor relative humidity | −1.77 | ±10 | 7.48 | 30 |
| P2 | Indoor temperature | −0.87 | ±10 | 4.64 | 30 |
| | Indoor relative humidity | −2.74 | ±10 | 8.67 | 30 |

characterize the indoor microclimate as meteorological data from meteorological agencies were used [80]. The output variables were the indoor temperature and the indoor relative humidity. Individual models were developed for each output variable (i.e., an MLP to estimate the indoor temperature, and another to estimate the indoor relative humidity). In addition, various MLPs were considered for the measurement points analysed. To obtain better estimate results, the output variable was logarithmically changed.

To develop the MLPs, a dataset is crucial for the training and testing. For this purpose, the case study was monitored to obtain a training dataset. Tests previously conducted in the church showed two very different points (Fig. 5): P1 corresponded to the zone of the altar and the sculpture of the Christ of the Good Death, and P2 corresponded to the nave of the church. The climate existing in P2 was homogeneous both in the central area of the church and in the transepts. These two points were monitored with HOBO U12-012 probes that measured the temperature and the relative humidity (Table 5). HOBO U12-012 fulfils the requirements set in both EN 15758 [81] (uncertainty of 0.5 °C) and EN 16242 [82] (uncertainty of 2.5%). In addition, the small size of the probes prevented users from stealing or misconfiguring it. These probes were placed in locations difficult to access (Fig. 5). The monitoring was carried out from 1 August 2017 (12:00 p.m.) to 24 July 2018 (22:00 p.m.), with a data acquisition interval of 1 h. Moreover, the outdoor temperature and the relative humidity were also monitored. For this purpose, the hourly data compiled by VAISALA HMP45D, a meteorological weather station that belongs to the Spanish Meteorological Agency (AEMET in Spanish), were used. VAISALA HMP45D has accuracy values that fulfil the limit values of both EN 15758 and EN 16242 (Table 5).

The dataset used for the training and testing of the MLPs was composed of the monitored data. As there were two measurement points, an MLP for P1 (MLP-P1) and another for P2 (MLP-P2) were developed. Moreover, the dataset was composed of observations from each hourly value recorded. The output variable corresponded to the hourly value of the indoor microclimate that each MLP aims to estimate. Thus, the MLP was used to estimate the time series of the indoor microclimate. The training and testing were performed by dividing the dataset (8,579 observations): 75% for the training, and 25% for the testing. A 10-fold cross validation was used to train MLPs, thus reducing the bias and the variance of the model [83]. At this point, the most

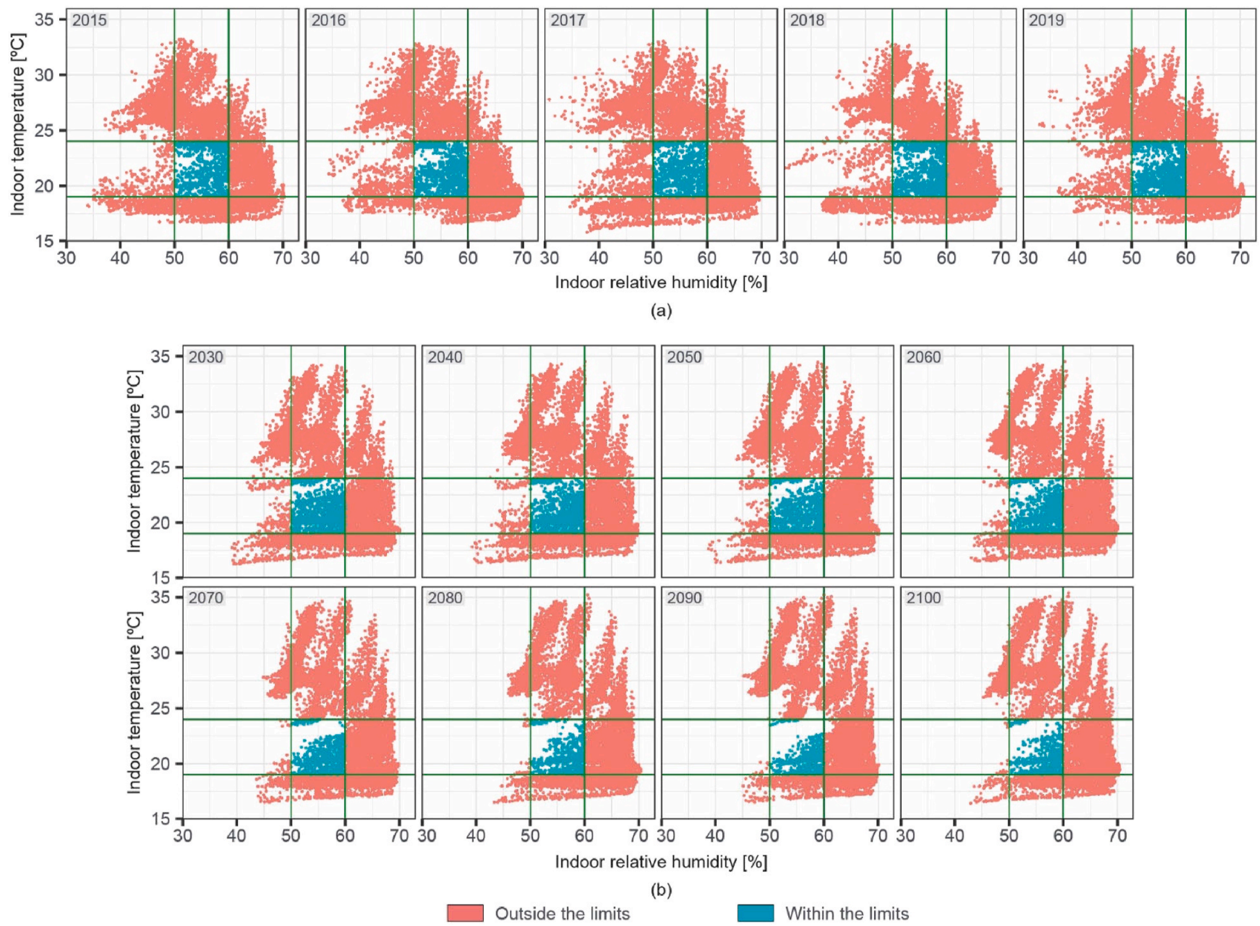


**Fig. 8.** Hourly values obtained each year in P1 of the indoor environmental variables, and delimitation of the optimal preservation zones for wooden objects. The green lines represent the upper and lower limits of the indoor temperature and the indoor relative humidity. (For interpretation of the references to colour in this figure legend, the reader is referred to the Web version of this article.)

appropriate architecture for each MLP was determined. For this purpose, the optimization of the MLPs were previously analysed by assessing architectures ranging between 1 and 2 hidden layers, with a number of neurons for each layer between 2 and 10.

To assess the performance of the MLPs, the criteria included in ASHRAE Guideline 14–2014 [84] to validate the simulation models were used. This validation process allows to verify that the estimate results are adjusted to the actual values with a margin of error. For this purpose, ASHRAE Guideline 14–2014 uses two error statistical parameters (Eqs. 13 and 14: the normalised mean bias error (NMBE) and the coefficient of variation of the root mean square error (CV(RMSE)). NMBE and CV(RMSE) are parameters like those traditionally used in data mining analyses, such as mean absolute error (MAE) or root mean square error (RMSE), so their use is suitable to validate the estimate models. Likewise, this aspect allowed comparisons to be made with the performance values obtained by studies based on energy simulation models. The limit values related to these parameters vary according to whether they are hourly or monthly limit values. The input and output variables of the MLPs are hourly, so the limit values are between −10% and 10% in NMBE and lower than 30% in CV(RMSE) [84,85].

$$NMBE = \frac{1}{\overline{m}} \cdot \frac{\sum_{i=1}^{n}(m_i - s_i)}{n-p} \tag{13}$$

$$CV(RMSE) = 100 \cdot \frac{1}{\overline{m}} \cdot \sqrt{\frac{\sum_{i=1}^{n}(m_i - s_i)^2}{n-p}} \tag{14}$$

After the MLPs of the indoor temperature and the indoor relative humidity of each point were obtained, the indoor environmental variables of temperature and relative humidity were estimated in the various scenarios. For the current scenario, the years 2015, 2016, 2017, 2018 and 2019 were analysed, and for the future scenario, each decade of the 21st century after the performance of this study was analysed. An hourly time serie of the outdoor environmental variables that were used as input in the MLPs (temperature, dew temperature, and relative humidity) was required. The data obtained by VAISALA HMP45D were also used to obtain outdoor hourly data between 2015 and 2019 (Fig. 6). The values of the distributions of the monitored outdoor climate variables were consistent with the type of climate in Seville. Thus, the maximum temperature values oscillated between 40.8 and 44.0 °C, with minimum values between 0.1 and 1.5 °C. The values of the quartiles oscillated between 12.7 and 13.5 °C in the first quartile (Q1), between 17.2 and 19.2 °C in the second quartile (Q2), and between 23.3 and 25.9 °C in the third quartile. The interquartile range was therefore similar in the temperature time series of the current scenario. In addition, the outdoor relative humidity had a similar trend in the similarity of the quartile values.

However, measured data were not available for the future scenarios, so estimates of the future climate were used. The A2 scenario was used as it is among the most unfavourable climate change scenarios developed by the Intergovernmental Panel on Climate Change [86–90]. This scenario considers a heterogeneous world with very marked demographic and economic increases, thus implying a temperature increase between 2 and 5.4 °C in 2100. Given its unfavourable characteristics, this scenario has been widely used to analyse the climate change impact on the built environment [86–90]. Moreover,

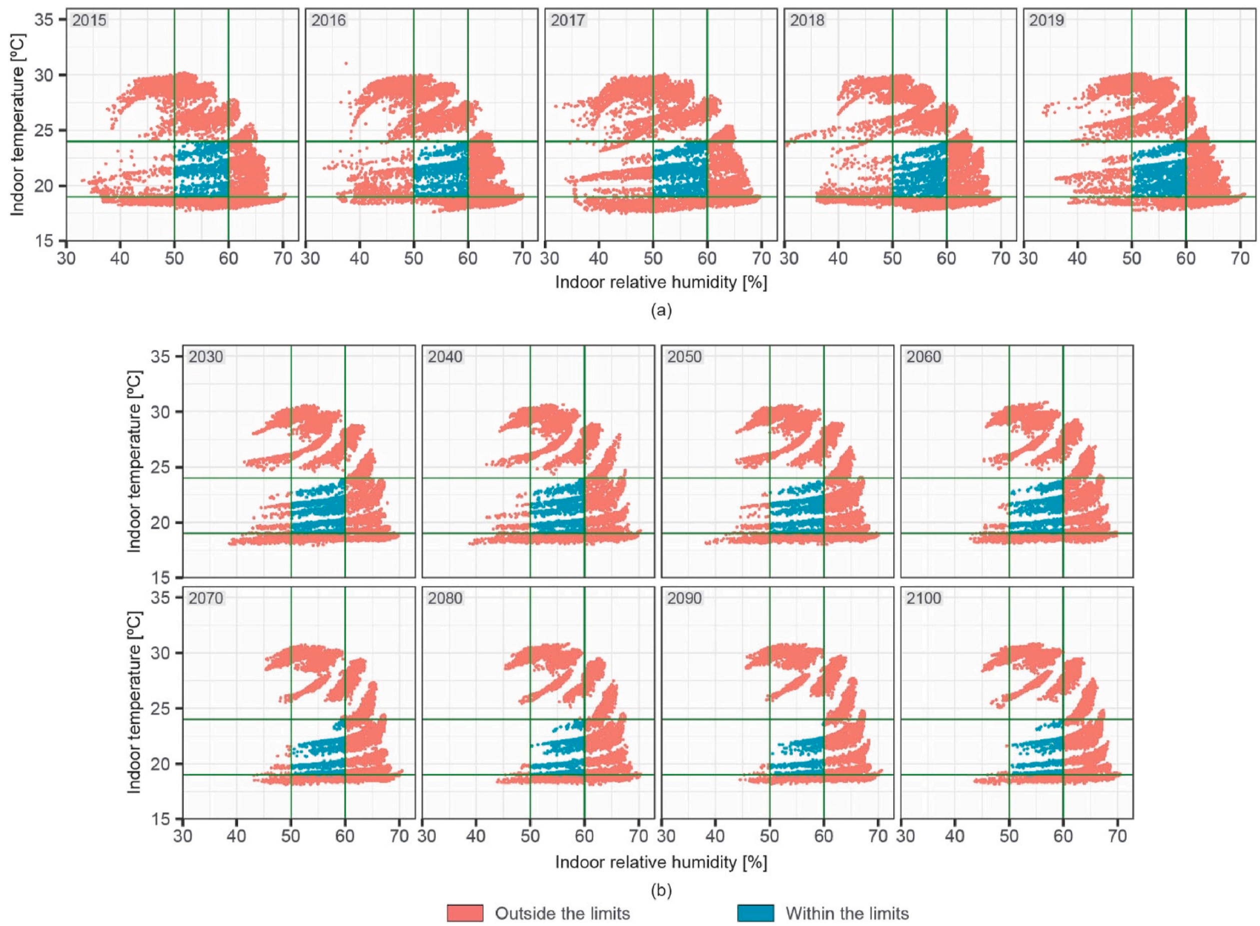


**Fig. 9.** Hourly values obtained each year in P2 of the indoor environmental variables and delimitation of the optimal preservation zones for wooden objects. The green lines represent the upper and lower limits of the indoor temperature and the indoor relative humidity. (For interpretation of the references to colour in this figure legend, the reader is referred to the Web version of this article.)

METEONORM was used to generate hourly climate data in the A2 scenario. METEONORM is a software made up of 8,325 weather stations spread all over the planet. With these references, METEONORM allows spatial interpolations and stochastic meteorological data to be generated [91]. Future time series are estimated by METEONORM using an average of the 18 climate models included in the 2007 report of the Intergovernmental Panel on Climate Change. The models used are averaged for the periods 2011–2030, 2046–2065, and 2080–2099. Through linear interpolations, METEONORM allows the values of each decade of the 21st century to be obtained. METEONORM obtained data in 2030, 2040, 2050, 2060, 2070, 2080, 2090 and 2100, so the evolution of the indoor microclimate in the church throughout the century was known in detail. These data were characterized by an increase in the values of the temperature quartiles. In this regard, while values of 14.5, 19.8 and 26 °C were obtained in 2030 in Q1, Q2, and Q3, respectively, these quartiles increased between 2.5 and 3.7 °C in 2100. With the MLPs, therefore, this study analysed the time series of the indoor microclimate in the church in 5 years of the current scenario and throughout the 21st century, thus obtaining the performance expected in the indoor microclimate with no improvement strategies.

## 3. Results and discussion

### 3.1. MLP performance

The performance of the MLPs was analysed before studying the indoor microclimate of the church. The analysis was based on the assessment of the statistical parameters considered in the result validation processes simulated by ASHRAE Guideline 14: NMBE and CV (RMSE). The determination coefficient was also assessed. As mentioned in the methodology section, the architecture of the MLPs oscillated between 1 and 2 hidden layers, analysing a combination of neurons that oscillated between 2 and 10 in each layer. In this optimization process of the architecture, it was detected that the architecture of 2 layers with 6 neurons in the first layer and 4 in the second layer obtained the best estimates: in the training phase, the determination coefficient was 95.54% in MLP-P1 (temperature), 89.40% in MLP-P1 (RH), 96.99% in MLP-P2 (temperature), and 90.98% in MLP-P2 (RH). Thanks to these results, satisfactory results of the determination coefficient were also obtained in the testing phase, with values that oscillated between 85.88% and 96.57%. However, the viability of the estimates could be assessed by fulfilling the error parameters established in ASHRAE Guideline 14. Fig. 7 shows the point clouds between the actual and the estimated values of the output variable of each MLP, and Table 6 shows the values obtained in NMBE and CV(RMSE). The values of NMBE and CV(RMSE) fulfilled the criteria established in ASHRAE Guideline 14, with an average distance to the closest limit value of 8.40% in NMBE and 23.445% in CV(RMSE). Nonetheless, some limitations were detected in the point clouds. Firstly, the estimated values for the indoor relative humidity presented a ceiling of 70.31% in P1 and 65.92% in P2 because of the low data density in the time series monitored in this range of values. Thus, values greater than 70% in P1 corresponded to 3.1% of the dataset, and values greater than 65% in P2 corresponded to 5.1%. Therefore, this lower density contributed to a worse estimate in this range of values. Secondly, no estimated values were obtained in the interval between 29.5 and 30 °C in P2 (i.e., the estimated values for this

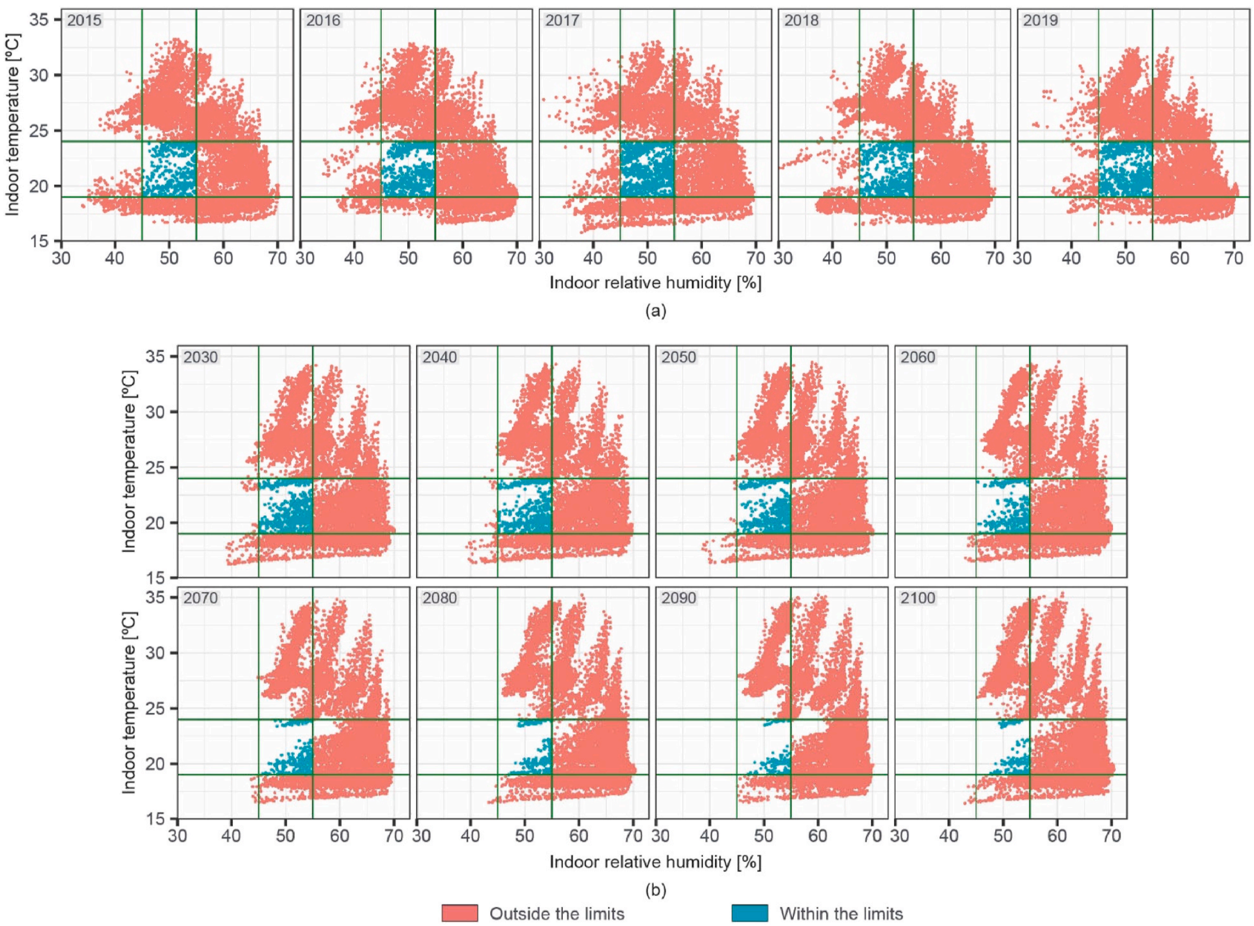


**Fig. 10.** Hourly values obtained each year in P1 of the indoor environmental variables and delimitation of the optimal preservation zones for paintings. The green lines represent the upper and lower limits of the indoor temperature and the indoor relative humidity. (For interpretation of the references to colour in this figure legend, the reader is referred to the Web version of this article.)

range of actual values were greater) because of the low density of actual data in this interval (0.83% of the observations in the dataset). However, the estimates obtained in this range were appropriate, with an average error of 0.75 °C. Despite these limitations, the performance obtained with the MLPs was acceptable. In this regard, the use of energy simulation models in other studies obtained performance values between 8% and 24% [18] and between 14.56% and 15% [12] in CV(RMSE). These values were greater than those obtained with the MLPs. The MLPs designed for the variables of temperature and relative humidity in P1 and P2 were therefore useful to make estimates according to the criteria established in ASHRAE Guideline 14. In addition, the MLPs could be used as a method to estimate the indoor values in view of the variation of the input variables.

### 3.2. Assessment of the performance index

The MLPs obtained appropriate performances to estimate the indoor environmental values. These methods were used to estimate the indoor microclimate both in the current scenario (i.e., 2015, 2016, 2017, 2018 and 2019) and in the future scenario (i.e., 2030, 2040, 2050, 2060, 2070, 2080, 2090 and 2100). On the other hand, the hourly data of the time series were used to assess the PI in the two main points of the church with the limit values established in the UNI 10829 (for both wooden objects and paintings). Figs. 8–11 show the hourly concentration values in each year within the appropriate preservation limits. The hourly concentration values within the appropriate environmental conditions corresponded to a fraction of the hours of the year, but temperature or relative humidity values outside the appropriate preservation limits were obtained in many hours of the year. However, the type of material and its limit values influenced the PI. Fig. 12 shows the PI values obtained in each years analysed, distinguishing in each line the value obtained by combining the measurement point and material. Thus, red points correspond to wooden objects, and blue points to paintings, while the continuous line corresponds to P1, and the dashed line to P2. The limit values for wooden objects obtained greater PI values than for paintings, with values oscillating between 0.85 and 6.15% in P1, and between 4.72 and 7.85% in P2. Despite the slight improvement of the wooden objects in comparison with the paintings, the conditions of the indoor microclimate were not appropriate to preserve the heritage elements. Thus, the constant actions taken to preserve the existing wooden sculptures are understandable. In this regard, the PI values in the current scenario (2015–2019) were as follows: (i) between 9.4 and 11.3% in the wooden objects in P1; (ii) between 10.5 and 12.7% in the wooden objects in P2; (iii) between 5.4 and 9.7% in the paintings in P1; and (iv) between 4.6 and 8% in the paintings in P2. These values were far from the minimum value recommended by Corgnati et al. [59]: 80% for the indoor environment. On the other hand, the PI will be progressively reduced inside the church throughout the 21st century because of the foreseeable climate change impact. In this regard, the PI values presented per decade an average decrease of 0.92% in the wooden objects and of 0.71% in the paintings, obtaining at the end of the century PI values between 6.6 and 6.8% in the wooden objects, and between 1.8 and 2.3% in paintings. This progressive decrease showed the vulnerability of the appropriate preservation of heritage elements. The variation in the outdoor climate would affect indoor microclimate. In cold climatic zones, this change covers a greater percentage of hours in the

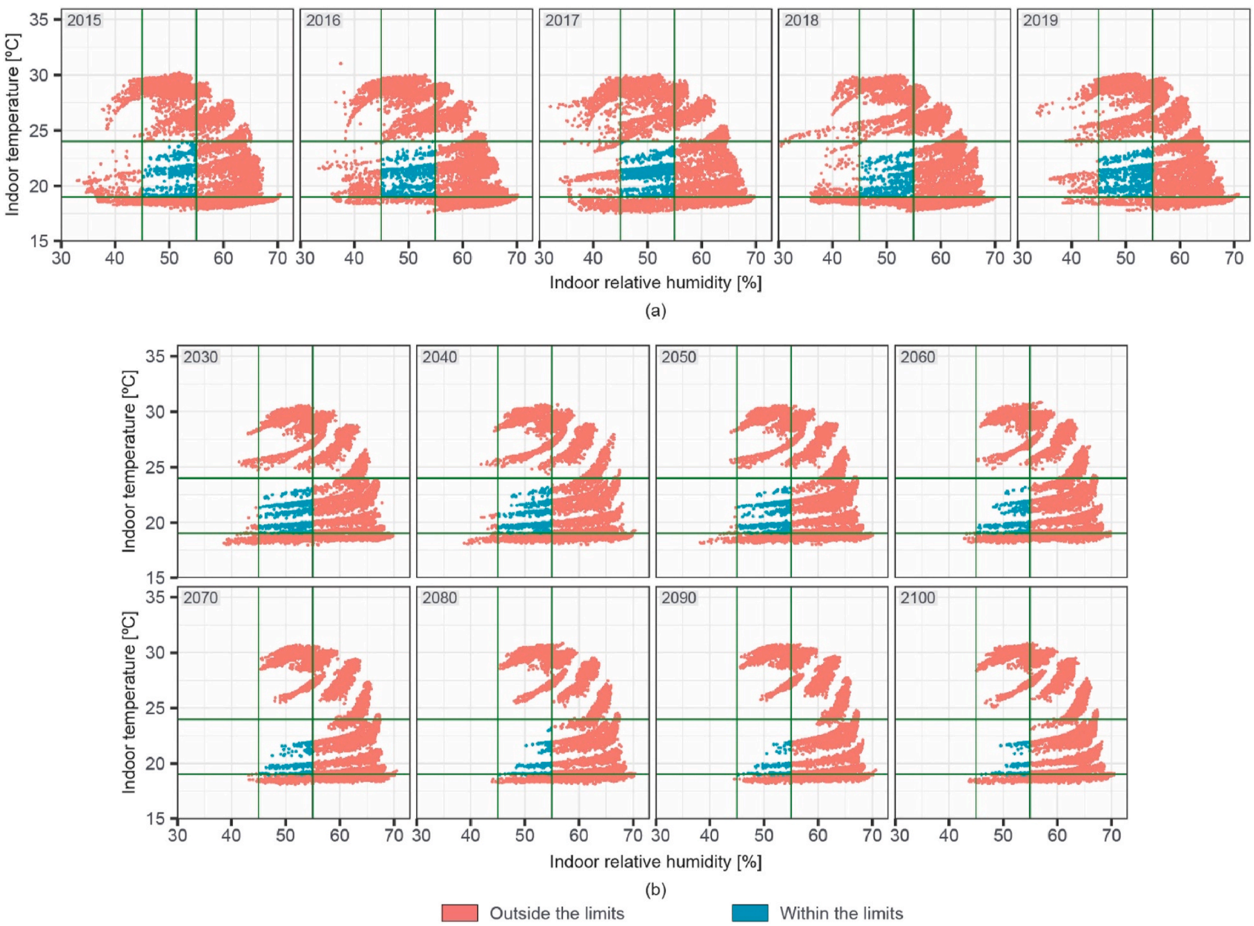


**Fig. 11.** Hourly values obtained each year in P2 of the indoor environmental variables and delimitation of the optimal preservation zones for paintings. The green lines represent the upper and lower limits of the indoor temperature and the indoor relative humidity. (For interpretation of the references to colour in this figure legend, the reader is referred to the Web version of this article.)

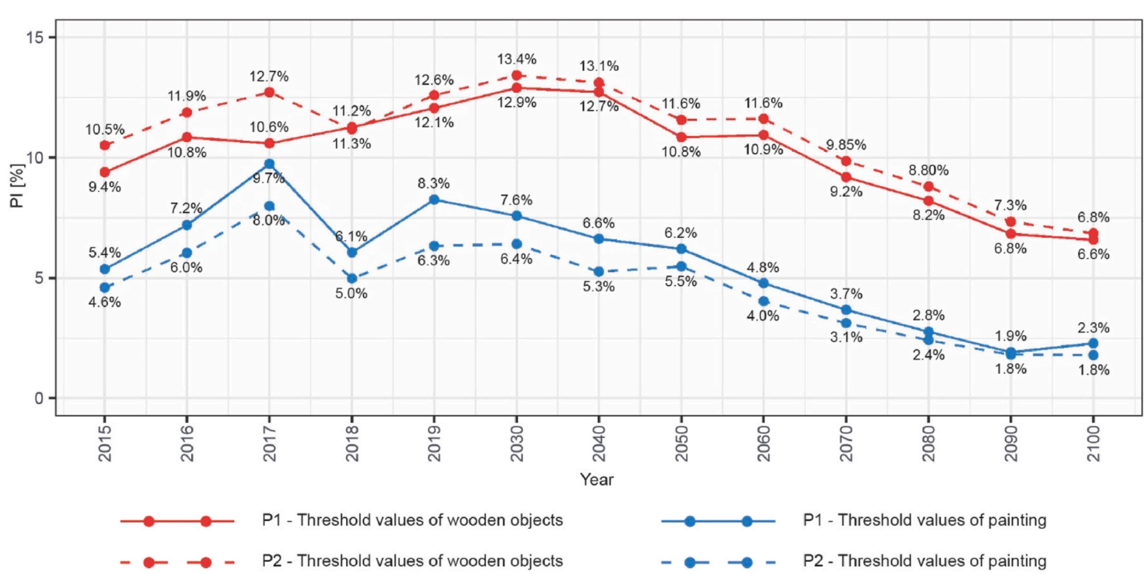


**Fig. 12.** PI evolution in each measurement point according to the type of material.

preservation thresholds [47]. However, many hours are outside the preservation thresholds in warm areas. This aspect becomes important if the indoor microclimate is already deficient in the current state since the displacement of the time series due to climate change could increase the preservation risk.

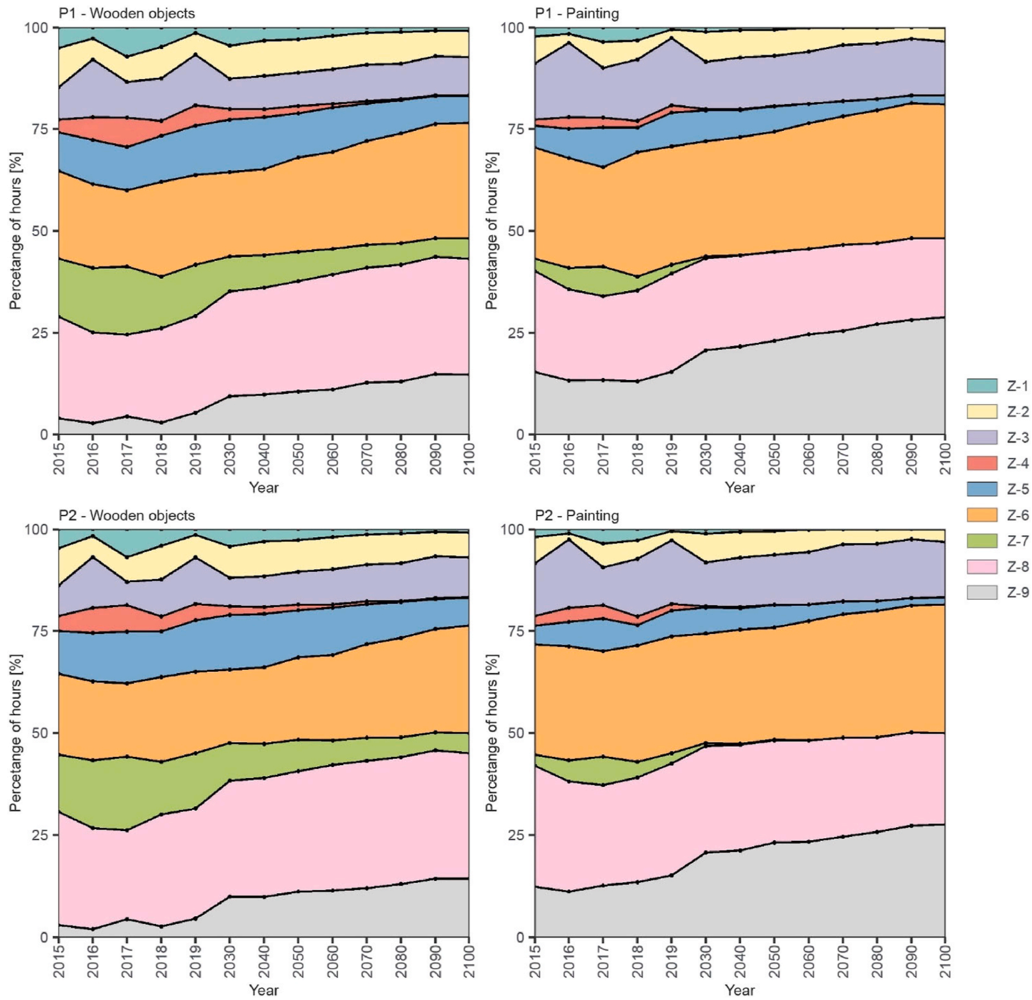


**Fig. 13.** Stacked area chart with the percentage of the hours of the year in the various preservation zones.

### 3.3. Assessment of the environmental treatment zones

Climate change is expected to worsen the indoor microclimate conditions in the historic buildings already presenting a deficient state in the current scenario. Consequently, actions should be taking in the indoor microclimate if there are low values in the PI, thus avoiding a progressive worsening throughout the 21st century. However, it is crucial to analyse the zones that are going to vary the annual hours outside the limit values. As mentioned in the methodology section, this study considered 9 environmental zones according to their location with respect to the preservation limits defined in UNI 10829 (with Z-5 being the zone which fulfilled the appropriate limits of temperature and relative humidity). Fig. 13 shows the distribution of the annual percentage of hours in the 9 zones. The percentage of hours varied both in the current and future scenario. In the current scenario, Z-1, Z-2, Z-7, and Z-8 obtained percentage reductions in the number of hours in those zones. Between 2015 and 2019, there was a reduction between 1.44 and 3.70% in Z-1, between 3.57 and 4.47% in Z-2, between 0.13 and 1.63% in Z-7, and between 0.78 and 2.23% in Z-8. Nonetheless, the oscillatory character of the outdoor climate implied that, in some of the years corresponding to the current scenario, the percentage of hours increased in these zones in comparison with the previous year, although the general tendency in the current scenario was the reduction of the percentage of hours. This reduction in Z-1, Z-2, Z-7, and Z-8 implied an increase in the other zones, with Z-3 being the zone with the greatest increase. Regarding climate change, the percentage of hours presented a clear reduction tendency in the zones with low relative humidity values (Z-1, Z-4, and Z-7). Thus, the percentage of hours in these zones was reduced between 0.34 and 3.58%, obtaining at the end of the century values that oscillated between 0.14 and 4.98% in the wooden objects, and between 0 and 0.15% in the paintings. Given this progressive tendency of obtaining greater temperature and relative humidity values in the hours of the year, concentrated in the right upper part of the plots of the point clouds (Figs. 8–11), the percentage of hours in Z-9 clearly increased between 4.44 and 5.32% in the wooden objects, and between 6.88 and 8.06% in the paintings. Likewise, there was a greater prevalence of the hours of the year in the other two zones with a relative humidity greater than the limit value recommended by UNI 10829 (Z-3 and Z-6), with increases between 1.89 and 8.44% in the wooden objects, and between 1.60 and 4.76% in the paintings. This aspect was already shown in the current scenario because the building presented a great concentration of hourly records with high relative humidity. The increase of the minimum values in the relative humidity time series in the future, together with the maintenance of the quartile values, increased the percentage of hours with high relative humidity. Therefore, it is expected that microclimates with high relative humidity will maintain this trend with the scenario analysed.

The variation of the percentage of hours should be complemented by analysing the distance of those hours with the optimal preservation values. Both the degree of severity of the hourly values in each zone and the demand level could therefore be analysed when establishing an environmental conditioning of the indoor space. Figs. 14–17 show the distance distributions obtained in each environmental treatment zone. Thus, climate change will vary the distances of each zone. Z-1, Z-4 and Z-

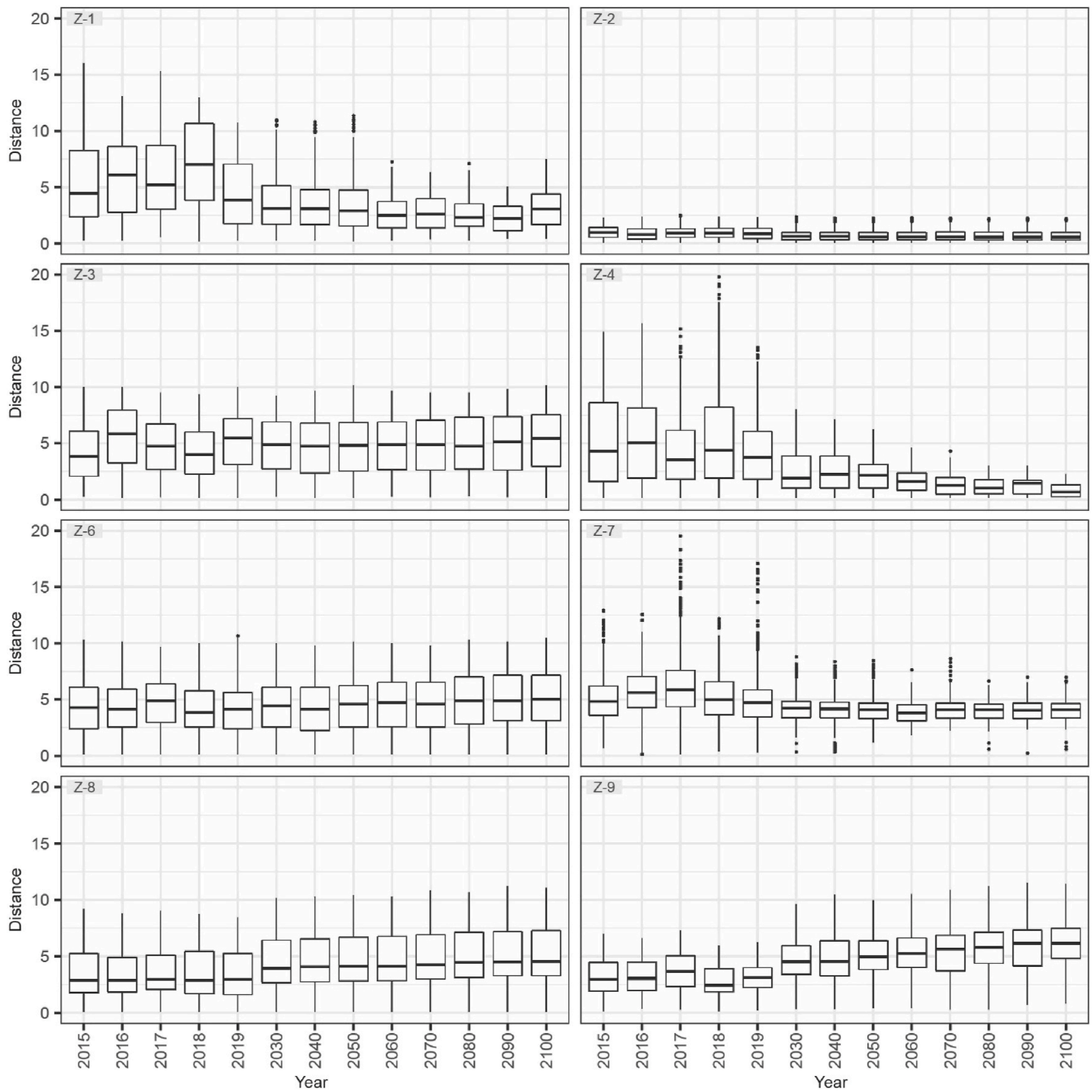


**Fig. 14.** Boxplots with the distance distributions obtained each year in P1 for the wooden objects.

7 presented a downward tendency throughout the 21st century: (i) in Z-1, the distributions presented a reduction at the end of the century between 0.10 and 0.46 in Q1, between 0.08 and 0.79 in Q2, and between 0.67 and 2.46 in Q3, and between 2.94 and 5.12 in the maximum values; (ii) in Z-4, the reductions were between 0.28 and 0.80 in Q1, between 0.78 and 1.23 in Q2, between 1.65 and 2.51 in Q3, and between 2.73 and 5.78 in the maximum values; and (iii) in Z-7, the reductions were between 0.02 and 1.82 in Q1, between 0.13 and 2.56 in Q2, between 0.22 and 4.25 in Q3, and between 1.83 and 4.50 in the maximum values. Regarding Z-4 and Z-7 in relation to the preservation of paintings, none of the hourly values were within these zones from 2050.

Despite the reduction of the distance in the zones with the least relative humidity, climate change increased the quartile values of the distance distributions in the zones with the greatest relative humidity (Z-3 and Z-6) and with the greatest temperature and relative humidity (Z-8 and Z-9). In Z-3, the variation was the least significant, with increases oscillating between 0.16 and 0.97 in Q1, between 0.36 and 1.00 in Q2, between 0.30 and 0.89 in Q3, and between 0.48 and 0.94 in the maximum values. Likewise, Z-8 presented an intermediate increase tendency (with values oscillating between 0.50 and 0.92 in Q1, between 0.48 and 0.65 in Q2, and between 0.48 and 1.06 in Q3), whereas Z-6 and Z-9 (corresponding to the zones with the greatest relative humidity) obtained the greatest increase values (between 0.58 and 2.36 in Q1, between 0.60 and 1.82 in Q2, between 0.90 and 1.87 in Q3, and between 0.49 and 1.90 in the maximum values). Thus, it is expected that climate change imply a progressive tendency of increasing the distribution of the distances in the zones with relative humidity greater than the limit value, particularly in the zone with the relative humidity and the temperature greater than the values recommended by the standard. In addition, climate change impact was lower in the zones with lower temperature values (e.g., Z-2). This aspect suggests the low effectiveness of implementing heating systems to improve the conditioning of the indoor microclimate throughout the 21st century. Some studies have reported a decrease in the heating energy demand in various regions of the European continent [51,86], so the heating strategies currently adopted in historic buildings are expected to be progressively less effective. The use of systems controlling the high temperature and the high relative humidity (through cooling and dehumidification processes) could obtain appropriate PI values according to the criteria established by Corgnati et al. [59] (Table 7). The use of cooling and dehumidification could obtain a PI between 92.48 and 96.78% at the end of the century, with an average progressive increase between 0.24 and 0.75%. Thus, the classification of the optimal conditions (A) by Corgnati et al. [59] would be obtain in the last quarter of the 21st

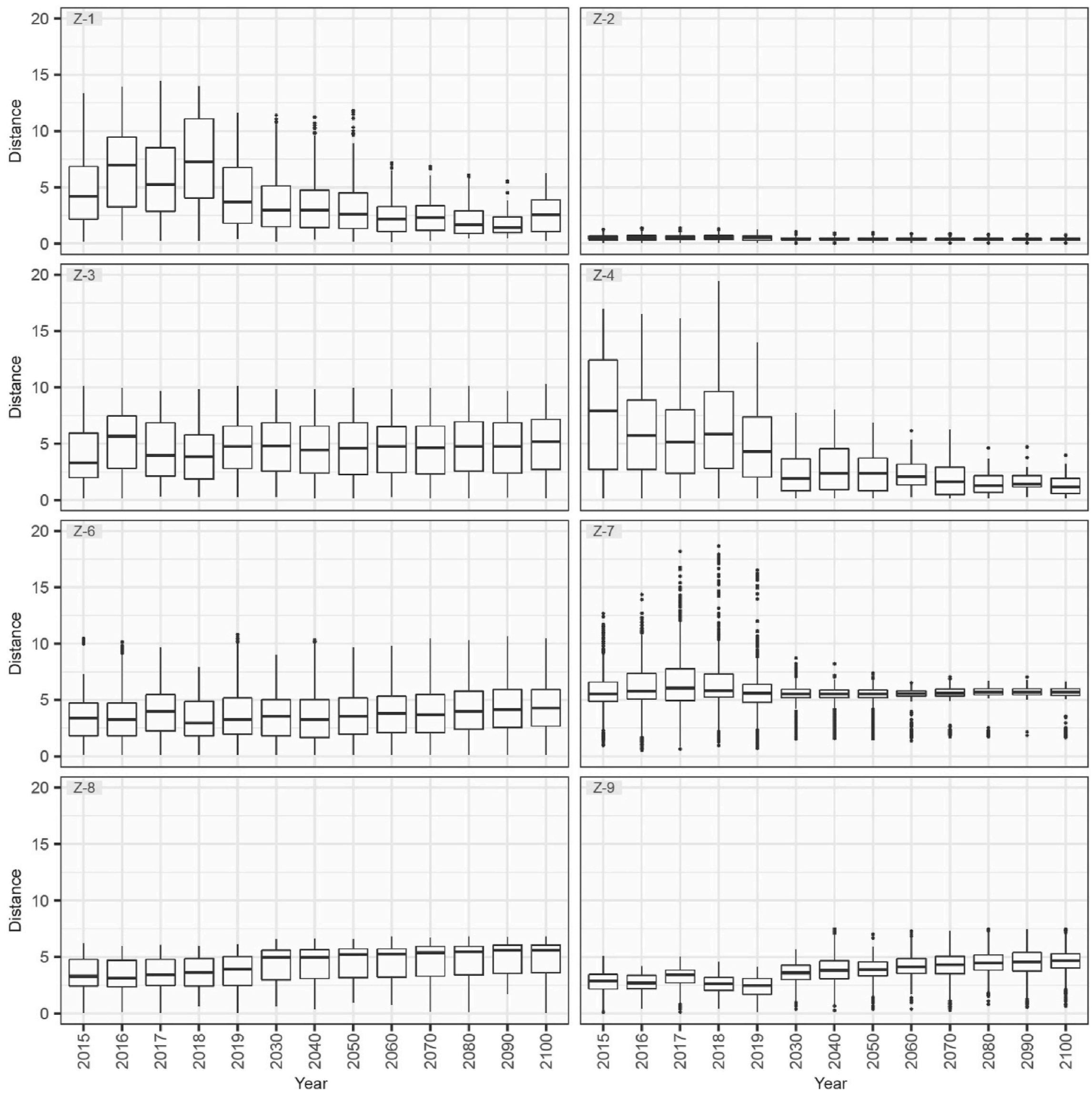


**Fig. 15.** Boxplots with the distance distributions obtained each year in P2 for the wooden objects.

century in the case of the wooden objects, and in the case of the paintings, that classification could be obtained in the current scenario. As a result, this type of strategies should be adopted in the historic buildings located in warm zones that present an inappropriate indoor microclimate in the current scenario to preserve heritage elements, thus guaranteeing an optimal preservation of the heritage elements for future generations.

Given the similarities of Seville's climate with other regions (e.g., southern European countries), the optimal HVAC strategies determined in the study could be applied. In this regard, a trend towards both a decrease in the use of heating systems and an increase in the use of cooling and dehumidification systems would allow better performance index values to be achieved. Likewise, the low value of observations detected in low temperature areas also suggests a progressive loss of the energy conservation measures based on the improvement of the envelope. Except when considering an improvement in the periodic thermal properties [92], the improvement of the thermal properties would not improve the performance index. In this regard, other studies focused on the effectiveness of effective building design measures have shown the limitations associated with effective designs traditionally used in warm regions [93,94]. The use of environmental conditioning strategies based on cooling and dehumidification would therefore allow appropriate performance to be achieved.

## 4. Conclusions

This study aimed to assess the climate change impact on the preservation risk of the heritage elements in historic buildings located in warm zones and under deficient environmental conditions in the current scenario. The characteristics of the indoor microclimate of a case study in Seville were analysed both in the current scenario (2015, 2016, 2017, 2018 and 2019) and throughout the 21st century (2030, 2040, 2050, 2060, 2070, 2080, 2090 and 2100). An estimate methodology of the hourly variables of each year was used through artificial neural networks, and a new analysis methodology of the environmental treatment zones based on the limits included in UNI 10829 was used. The following conclusions can be drawn according to the results obtained:

- The use of multilayer perceptrons could be an appropriate methodology to estimate the indoor microclimate in view of the variation of the outdoor variables, without using simulation models. The results obtained in NMBE and CV(RMSE) were satisfactory according to the criteria established by ASHRAE Guideline 14, with determination

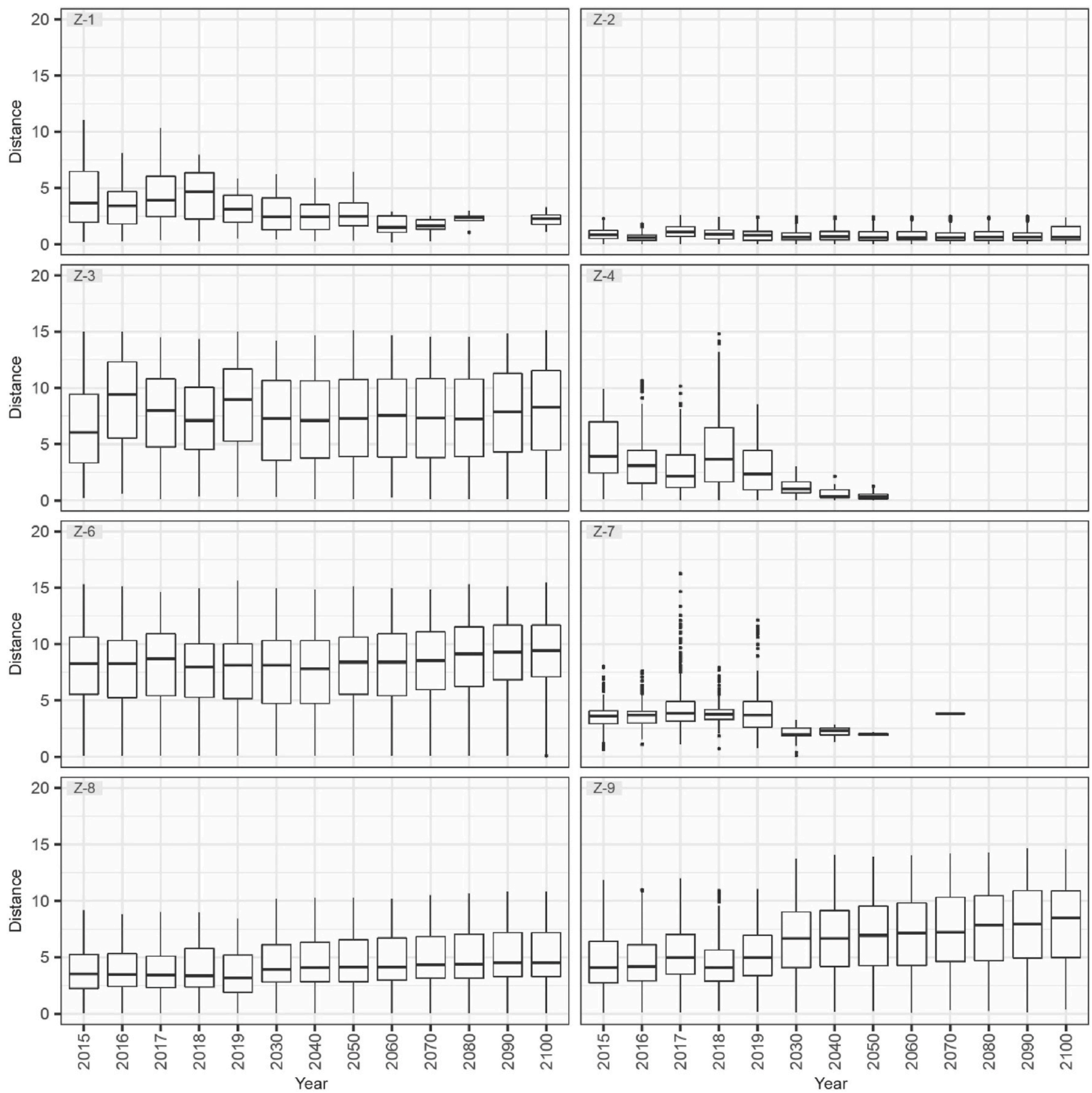


**Fig. 16.** Boxplots with the distance distributions obtained each year in P1 for the paintings.

coefficients between 85.88 and 96.99% in the training and testing phases.

- The PI in historic buildings with a deficient environmental climate could be very low. In the case study analysed, the performance index in the current scenario obtained values between 4.6 and 12.71% according to the type of material. These values, which are far from the minimum recommendation (80%), constitute an inappropriate environmental climate, as well as an excessive risk to preserve heritage elements. Moreover, climate change is expected to progressively reduce the performance index in this type of case studies. Thus, if current conditions are not appropriate, the preservation risk in heritage elements will be progressively increased throughout the 21st century.
- Moreover, climate change effect will not just reduce the performance index, but also vary the strategies to be adopted in the hours in which the environmental conditions are outside the preservation limits. For this purpose, the analysis of the environmental treatment zones, which was based on both the concepts of the percentage of hours (in an application similar to the performance index) and the distance to the optimal preservation point, reflected that the zones most influenced by climate change will be those related to a high relative humidity and those with the combinations of high temperature with a relative humidity in an appropriate preservation interval. This is a direct consequence of climate change effect that will imply a lower severity of the environmental conditioning zones with low temperature and low relative humidity, so there is a need for establishing environmental conditioning measures based on the use of cooling and dehumidification strategies.

To conclude, the results of this study are of interest to design appropriate environmental preservation strategies for the heritage elements of historic buildings in warm climate zones. First, the analysis methodology (based on both the use of artificial neural networks and the analysis of environmental treatment zones) characterizes the environmental hourly values of various climate scenarios and defines the most appropriate type of strategy (cooling, heating, humidification or dehumidification). Thus, this is a very useful methodology for curators, architects, and environmental engineers to assess the indoor microclimate in historic buildings. Moreover, the results of this study are of interest to develop financing policies to preserve historic buildings in warm climate zones. These results have shown that the most appropriate conditioning strategies to reduce the climate change impact should be based on the use of dehumidification and cooling strategies. Nonetheless, this research does not consider the possible impact on both energy

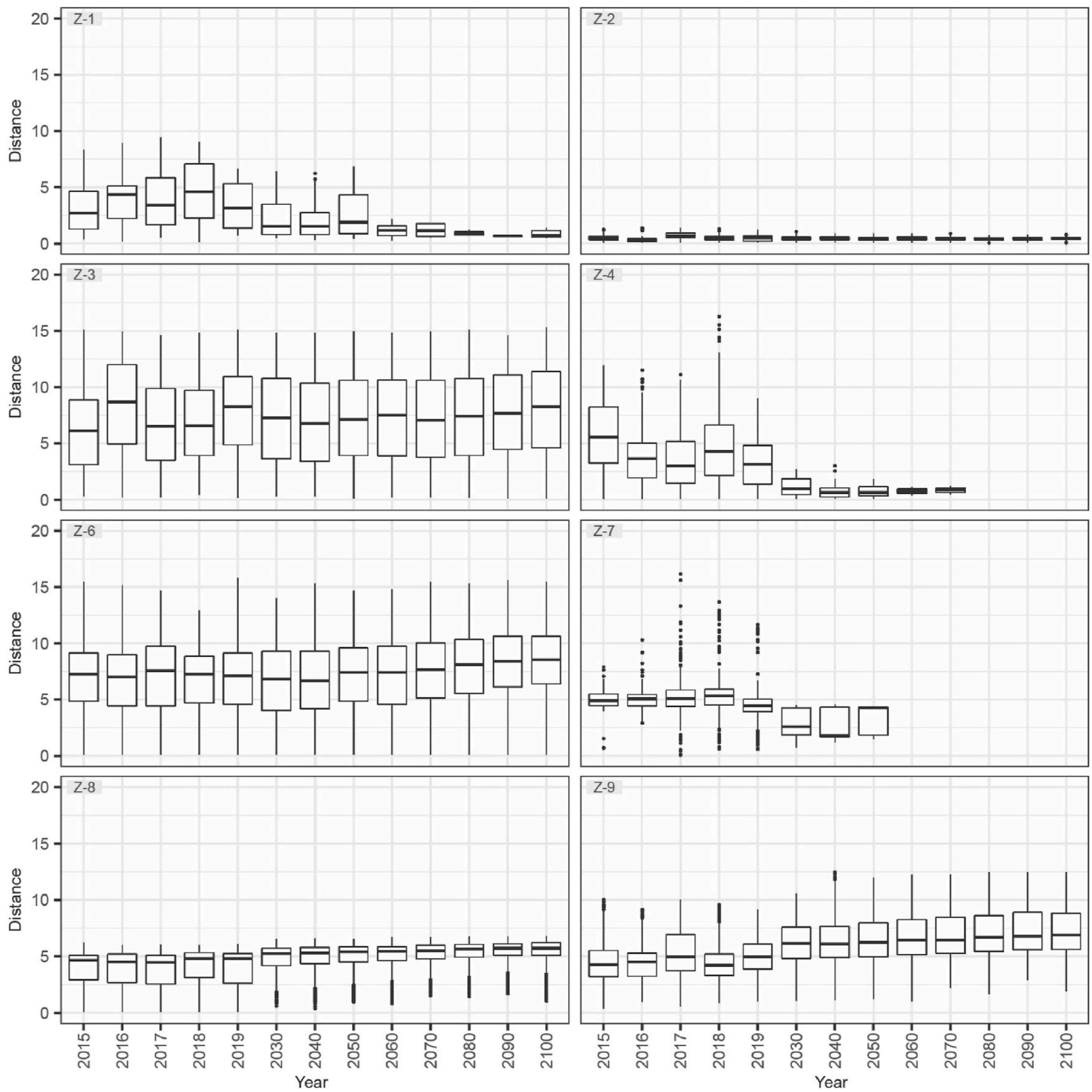


**Fig. 17.** Boxplots with the distance distributions obtained each year in P2 for the paintings.

**Table 7**
PI obtained with cooling and dehumidification strategies. The respective class according to the assessment method by Corgnati et al. [59] is also indicated.

| Year | PI [%] | | | |
|---|---|---|---|---|
| | P1 | | P2 | |
| | Wooden objects | Paintings | Wooden objects | Paintings |
| 2015 | 82.10 (C) | 89.60 (B) | 82.49 (C) | 89.16 (B) |
| 2016 | 86.52 (B) | 93.33 (A) | 87.00 (B) | 94.03 (A) |
| 2017 | 79.36 | 87.60 (B) | 80.58 (C) | 87.32 (B) |
| 2018 | 83.78 (C) | 90.45 (A) | 83.95 (C) | 90.54 (A) |
| 2019 | 88.24 (B) | 95.50 (A) | 89.03 (B) | 95.59 (A) |
| 2030 | 84.75 (C) | 91.15 (A) | 85.87 (B) | 91.52 (A) |
| 2040 | 86.06 (B) | 92.31 (A) | 86.74 (B) | 92.65 (A) |
| 2050 | 87.04 (B) | 92.89 (A) | 88.14 (B) | 93.54 (A) |
| 2060 | 88.77 (B) | 94.01 (A) | 89.41 (B) | 94.33 (A) |
| 2070 | 90.26 (A) | 95.62 (A) | 90.62 (A) | 96.21 (A) |
| 2080 | 90.78 (A) | 96.02 (A) | 91.35 (A) | 96.38 (A) |
| 2090 | 92.69 (A) | 97.19 (A) | 93.05 (A) | 97.48 (A) |
| 2100 | 92.48 (A) | 96.47 (A) | 92.87 (A) | 96.78 (A) |

consumption and carbon dioxide emissions by using these two strategies. For this reason, further steps should be focused on both the quantification of energy consumption by using dehumidification and cooling strategies and the possible implications for the decarbonisation goals predicted by the European Union. Likewise, this study does not consider the possible implications of the environmental control to preserve users' thermal comfort. Further studies should address this issue to guarantee a suitable indoor microclimate through the various uses predicted for HVAC systems according to EN 15759-1.

## Declaration of competing interest

The authors declare that they have no known competing financial interests or personal relationships that could have appeared to influence the work reported in this paper.

## Acknowledgement

This research has been funded by the "Consejería de Economía, Conocimiento, Empresas y Universidad de la Junta de Andalucía" through a postdoctoral research programme at University of Sevilla.

## References


[1] M.A. Vecco, Definition of cultural heritage: from the tangible to the intangible, J. Cult. Herit. 11 (2010) 321–324, https://doi.org/10.1016/j.culher.2010.01.006.
[2] J. Fu, J. Zhou, Y. Deng, Heritage values of ancient vernacular residences in traditional villages in western Hunan, China: spatial patterns and influencing factors, Build. Environ. (2021) 188, https://doi.org/10.1016/j.buildenv.2020.107473.
[3] M. Krebs, K. Schmidt-Hebbel, Patrimonio cultural: aspectos económicos y políticas de Protección. *Perspectivas en política*, Economía y Gestión 2 (1999) 207–245.
[4] R. Vicente, T.M. Ferreira, J.A.R. Mendes da Silva, Supporting urban regeneration and building refurbishment. Strategies for building appraisal and inspection of old building stock in city centres, J. Cult. Herit. 16 (2015) 1–14, https://doi.org/10.1016/j.culher.2014.03.004.
[5] E. Lucchi, Review of preventive conservation in museum buildings, J. Cult. Herit. 29 (2018) 180–193.
[6] D. Camuffo, Microclimate for Cultural Heritage, Elsevier, 1998. ISBN 0080536530.
[7] G. Pavlogeorgatos, Environmental parameters in museums, Build. Environ. 38 (2003) 1457–1462, https://doi.org/10.1016/S0360-1323(03)00113-6.
[8] L. Samek, A. de Maeyer-Worobiec, Z. Spolnik, L. Bencs, V. Kontozova, Ł. Bratasz, R. Kozłowski, R. van Grieken, The impact of electric overhead radiant heating on the indoor environment of historic churches, J. Cult. Herit. 8 (2007) 361–369, https://doi.org/10.1016/j.culher.2007.03.006.
[9] N. Aste, S. della Torre, R.S. Adhikari, M. Buzzetti, C. del Pero, F. Leonforte, M. Manfren, Sustainable church heating: the Basilica Di Collemaggio case-study, Energy Build. 116 (2016) 218–231, https://doi.org/10.1016/j.enbuild.2016.01.008.
[10] H.E. Silva, F.M.A. Henriques, The impact of tourism on the conservation and IAQ of cultural heritage: the case of the Monastery of Jerónimos (Portugal), Build. Environ. (2021) 190, https://doi.org/10.1016/j.buildenv.2020.107536.
[11] M.J. Varas-Muriel, R. Fort, M.I. Martínez-Garrido, A. Zornoza-Indart, P. López-Arce, Fluctuations in the indoor environment in Spanish rural churches and their effects on heritage conservation: hygro-thermal and CO2 conditions monitoring, Build. Environ. 82 (2014) 97–109, https://doi.org/10.1016/j.buildenv.2014.08.010.
[12] T. de Rubeis, I. Nardi, M. Muttillo, D. Paoletti, The restoration of severely damaged churches – implications and opportunities on cultural heritage conservation, thermal comfort and energy efficiency, J. Cult. Herit. 43 (2020) 186–203, https://doi.org/10.1016/j.culher.2019.11.008.
[13] D. Camuffo, The friendly heating project and the conservation of the cultural heritage preserved in churches, in: Developments in Climate Control of Historic Buildings, vols. 7–12, Fraunhofer IRB Verlag, Stuttgart, 2011.
[14] E. Lucchi, Environmental risk management for museums in historic buildings through an innovative approach: a case study of the pinacoteca Di Brera in milan (Italy), Sustainability 12 (2020), https://doi.org/10.3390/su12125155.
[15] M.J. Varas-Muriel, M.I. Martínez-Garrido, R. Fort, Monitoring the thermal-hygrometric conditions induced by traditional heating systems in a historic Spanish church (12th-16th C), Energy Build. 75 (2014) 119–132.
[16] C. Bonacina, P. Baggio, F. Cappelletti, P. Romagnoni, A.G. Stevan, The Scrovegni Chapel: the results of over 20 Years of indoor climate monitoring, Energy Build. 95 (2015) 144–152, https://doi.org/10.1016/j.enbuild.2014.12.018.
[17] C. Cornaro, V.A. Puggioni, R.M. Strollo, Dynamic simulation and on-site measurements for energy retrofit of complex historic buildings: villa Mondragone case study, Journal of Building Engineering 6 (2016) 17–28, https://doi.org/10.1016/j.jobe.2016.02.001.
[18] C.M. Muñoz González, A.L. León Rodríguez, R. Suárez Medina, J. Ruiz Jaramillo, Effects of future climate change on the preservation of artworks, thermal comfort and energy consumption in historic buildings, Appl. Energy (2020) 276, https://doi.org/10.1016/j.apenergy.2020.115483.
[19] M. Napp, T. Kalamees, Energy use and indoor climate of conservation heating, dehumidification and adaptive ventilation for the climate control of a mediaeval church in a cold climate, Energy Build. 108 (2015) 61–71, https://doi.org/10.1016/j.enbuild.2015.08.013.
[20] M.J. Varas-Muriel, R. Fort, Microclimatic monitoring in an historic church fitted with modern heating: implications for the preventive conservation of its cultural heritage, Build. Environ. 145 (2018) 290–307, https://doi.org/10.1016/j.buildenv.2018.08.060.
[21] N. Aste, R.S. Adhikari, M. Buzzetti, S. della Torre, C. del Pero, H.E. Huerto C, F. Leonforte, Microclimatic monitoring of the Duomo (milan Cathedral): risks-based analysis for the conservation of its cultural heritage, Build. Environ. 148 (2019) 240–257, https://doi.org/10.1016/j.buildenv.2018.11.015.
[22] T. Cardinale, G. Rospi, N. Cardinale, The influence of indoor microclimate on thermal comfort and conservation of artworks: the case study of the Cathedral of Matera (south Italy), in: Proceedings of the Energy Procedia, vol. 59, Elsevier Ltd, 2014, pp. 425–432.
[23] D. Camuffo, G. Sturaro, A. Valentino, M. Camuffo, The conservation of artworks and hot air heating systems in churches: are they compatible? The case of Rocca Pietore, Italian alps, Stud. Conserv. 44 (1999) 209–216, https://doi.org/10.1179/sic.1999.44.3.209.
[24] H.E. Silva, F.M.A. Henriques, Microclimatic analysis of historic buildings: a new methodology for temperate climates, Build. Environ. 82 (2014) 381–387, https://doi.org/10.1016/j.buildenv.2014.09.005.
[25] W. Anaf, O. Schalm, Climatic quality evaluation by peak analysis and segregation of low-, mid-, and high-frequency fluctuations, applied on a Historic Chapel, Build. Environ. 148 (2019) 286–293, https://doi.org/10.1016/j.buildenv.2018.11.018.
[26] C. Basto, L. Pelà, R. Chacón, Open-source digital technologies for low-cost monitoring of historical constructions, J. Cult. Herit. 25 (2017) 31–40, https://doi.org/10.1016/j.culher.2016.12.003.
[27] F.J. García-Diego, M. Zarzo, Microclimate monitoring by multivariate statistical control: the renaissance frescoes of the cathedral of Valencia (Spain), J. Cult. Herit. 11 (2010) 339–344, https://doi.org/10.1016/j.culher.2009.06.002.
[28] Z. Spolnik, A. Worobiec, L. Samek, L. Bencs, K. Belikov, R. van Grieken, Influence of different types of heating systems on particulate air pollutant deposition: the case of churches situated in a cold climate, J. Cult. Herit. 8 (2007) 7–12, https://doi.org/10.1016/j.culher.2006.09.003.
[29] S.E. Chatoutsidou, L. Mašková, L. Ondráčková, J. Ondráček, M. Lazaridis, J. Smolík, Modeling of the aerosol infiltration characteristics in a cultural heritage building: the Baroque library Hall in prague, Build. Environ. 89 (2015) 253–263, https://doi.org/10.1016/j.buildenv.2015.02.029.
[30] L. Bencs, Z. Spolnik, A. Worobiec, L. Samek, B.A.H.G. Jütte, R. van Grieken, Effects of IR heating on distribution and transport of gaseous air pollutants in urban and mountain churches in Poland, J. Cult. Herit. 36 (2019) 200–209, https://doi.org/10.1016/j.culher.2018.09.007.
[31] T. Kalamees, A. Väli, L. Kurik, M. Napp, E. Arümagi, U. Kallavus, The influence of indoor climate control on risk for damages in naturally ventilated historic churches in cold climate, Int. J. Architect. Herit. 10 (2016) 486–498, https://doi.org/10.1080/15583058.2014.1003623.
[32] M. Andretta, F. Coppola, L. Seccia, Investigation on the interaction between the outdoor environment and the indoor microclimate of a historical library, J. Cult. Herit. 17 (2016) 75–86, https://doi.org/10.1016/j.culher.2015.07.002.
[33] M.P. Diulio, P. Mercader-Moyano, A.F. Gómez, The influence of the envelope in the preventive conservation of books and paper records. Case study: libraries and archives in La Plata, Argentina, Energy Build. 183 (2019) 727–738, https://doi.org/10.1016/j.enbuild.2018.11.048.
[34] Torres-González, M.; Alejandre, F.J.; Flores-Alés, V.; Calero-Castillo, A.I.; Blasco-López, F.J. Analysis of the state of conservation of historical plasterwork through visual inspection and non-destructive tests. The case of the upper frieze of the Toledanos room (the royal alcázar of Seville, Spain). Journal of Building Engineering 2021, 102314, doi:10.1016/j.jobe.2021.102314.
[35] F. Sciurpi, C. Carletti, G. Cellai, L. Pierangioli, Environmental monitoring and microclimatic control strategies in "La Specola" museum of florence, Energy Build. 95 (2015) 190–201, https://doi.org/10.1016/j.enbuild.2014.10.061.
[36] F.J. García-Diego, E. Verticchio, P. Beltrán, A. Siani, Assessment of the minimum sampling frequency to avoid measurement redundancy in microclimate field surveys in museum buildings, Sensors 16 (2016), https://doi.org/10.3390/s16081291.
[37] G. Litti, A. Audenaert, K. Fabbri, Indoor microclimate quality (IMQ) certification in heritage and museum buildings: the case study of vleeshuis museum in antwerp, Build. Environ. 124 (2017) 478–491, https://doi.org/10.1016/j.buildenv.2017.08.013.
[38] E. Lucchi, Multidisciplinary risk-based analysis for supporting the decision making process on conservation, energy efficiency, and human comfort in museum buildings, J. Cult. Herit. 22 (2016) 1079–1089.
[39] E. Schito, P. Conti, D. Testi, Multi-objective optimization of microclimate in museums for concurrent reduction of energy needs, visitors' discomfort and artwork preservation risks, Appl. Energy 224 (2018) 147–159, https://doi.org/10.1016/j.apenergy.2018.04.076.
[40] C. Manfriani, G. Gualdani, G. Goli, B. Carlson, A.R. Certo, P. Mazzanti, M. Fioravanti, The contribution of IoT to the implementation of preventive conservation according to European standards: the case study of the "cannone" violin and its historical copy, Sustainability 13 (2021) 1900, https://doi.org/10.3390/su13041900.
[41] V. Rajčić, A. Skender, D. Damjanović, An innovative methodology of assessing the climate change impact on cultural heritage, Int. J. Architect. Herit. 12 (2018) 21–35, https://doi.org/10.1080/15583058.2017.1354094.
[42] C. Sabbioni, P. Brimblecombe, M. Cassar, The Atlas of Climate Change Impact on European Cultural Heritage: Scientific Analysis and Management Strategies, Anthem Press, 2010. ISBN 1843317982.
[43] G. Matthews, Y. Smith, G. Knowles, Disaster management in archives, libraries and museums: an international overview, Alexandria 19 (2007) 1–22, https://doi.org/10.1177/095574900701900102.
[44] G. Sevieri, C. Galasso, Typhoon risk and climate-change impact assessment for cultural heritage asset roofs, Struct. Saf. (2021) 91, https://doi.org/10.1016/j.strusafe.2020.102065.
[45] F. García Sánchez, H. García Sánchez, C. Ribalaygua, Cultural heritage and sea level rise threat: risk assessment of coastal fortifications in the canary islands, J. Cult. Herit. 44 (2020) 211–217, https://doi.org/10.1016/j.culher.2020.02.005.
[46] P. Ezcurra, I.C. Rivera-Collazo, An assessment of the impacts of climate change on Puerto Rico's cultural heritage with a case study on sea-level rise, J. Cult. Herit. 32 (2018) 198–209, https://doi.org/10.1016/j.culher.2018.01.016.
[47] E. Verticchio, F. Frasca, F.J. Garcìa-Diego, A.M. Siani, Investigation on the use of passive microclimate frames in view of the climate change scenario, Climate 7 (2019), https://doi.org/10.3390/cli7080098.
[48] A.J. Prieto, K. Verichev, M. Carpio, Heritage, resilience and climate change: a fuzzy logic application in timber-framed Masonry buildings in valparaíso, Chile, Build. Environ. (2020) 174, https://doi.org/10.1016/j.buildenv.2020.106657.
[49] A.J. Prieto, K. Verichev, A. Silva, J. de Brito, On the impacts of climate change on the functional deterioration of heritage buildings in south Chile, Build. Environ. (2020) 183, https://doi.org/10.1016/j.buildenv.2020.107138.
[50] A.J. Prieto, A. Silva, J. de Brito, J.M. Macías-Bernal, F.J. Alejandre, The influence of pathological situations on churches' functionality: an approach based on

historical records, Int. J. Architect. Herit. 11 (2017) 566–587, https://doi.org/10.1080/15583058.2016.1272011.
[51] D. Bienvenido-Huertas, D. Sánchez-García, C. Rubio-Bellido, M.J. Oliveira, Influence of adaptive energy saving techniques on office buildings located in cities of the iberian peninsula, Sustain. Cities Soc. 53 (2020) 101944, https://doi.org/10.1016/j.scs.2019.101944.
[52] D. Bienvenido-Huertas, C. Rubio-Bellido, A. Pérez-Fargallo, J.A. Pulido-Arcas, Energy saving potential in current and future world built environments based on the adaptive comfort approach, J. Clean. Prod. 249 (2020), https://doi.org/10.1016/j.jclepro.2019.119306.
[53] C.M. Muñoz-González, A.L. León-Rodríguez, J. Navarro-Casas, Air conditioning and passive environmental techniques in historic churches in Mediterranean climate. A proposed method to assess damage risk and thermal comfort pre-intervention, simulation-based, Energy Build. 130 (2016) 567–577.
[54] V. Pérez-Andreu, C. Aparicio-Fernández, A. Martínez-Ibernón, J.L. Vivancos, Impact of climate change on heating and cooling energy demand in a residential building in a Mediterranean climate, Energy 165 (2018) 63–74, https://doi.org/10.1016/j.energy.2018.09.015.
[55] A. Jiang, X. Liu, E. Czarnecki, C. Zhang, Hourly weather data projection due to climate change for impact assessment on building and infrastructure, Sustain. Cities Soc. 50 (2019), 101688, https://doi.org/10.1016/j.scs.2019.101688.
[56] Pepe Becerra Leyendas de Sevilla: Capilla de La Universidad, -I.
[57] The Government of Spain, Royal Decree 732/2019, of December 20, Which Modifies the Technical Building Code, Approved by Royal Decree 314/2006, of March 17, 2019.
[58] Ente Nazionale Italiado di Unificazione, in: UNI 10829: 1999-Beni Di Interesse Storico e Artistico–Condizioni Ambientali Di Conservazione-Misurazione, Analisi, 1999.
[59] S.P. Corgnati, V. Fabi, M. Filippi, A methodology for microclimatic quality evaluation in museums: application to a temporary exhibit, Build. Environ. 44 (2009) 1253–1260, https://doi.org/10.1016/j.buildenv.2008.09.012.
[60] S.P. Corgnati, M. Filippi, Assessment of thermo-hygrometric quality in museums: method and in-field application to the " Duccio Di buoninsegna" exhibition at Santa Maria Della Scala (Siena, Italy), J. Cult. Herit. 11 (2010) 345–349, https://doi.org/10.1016/j.culher.2009.05.003.
[61] K. Fabbri, M. Pretelli, Heritage buildings and historic microclimate without HVAC technology: Malatestiana library in Cesena, Italy, UNESCO memory of the world, Energy Build. 76 (2014) 15–31, https://doi.org/10.1016/j.enbuild.2014.02.051.
[62] F. Sciurpi, A. Ghelli, L. Pierangioli, "La Specola" museum in florence: environmental monitoring and building energy simulation, Procedia Struct. Integr. 29 (2020) 16–24, https://doi.org/10.1016/j.prostr.2020.11.134.
[63] UCLA Energy Design Tools Group, *Climate Consultant® Software V*. 6, 0 Software Program© Regents of the University of California, 2018.
[64] Martini, R.; Carvalho, J.; Arêde, A.; Varum, H. Validation of the use of non-destructive methods of assessing stone Masonry by artificial neural networks. Journal of Building Engineering 2021, 102469, doi:10.1016/j.jobe.2021.102469.
[65] G. Barone, P. Mazzoleni, G.V. Spagnolo, S. Raneri, Artificial neural network for the provenance study of archaeological ceramics using clay sediment database, J. Cult. Herit. 38 (2019) 147–157, https://doi.org/10.1016/j.culher.2019.02.004.
[66] A. Liguori, R. Markovic, T.T.H. Dam, J. Frisch, C. van Treeck, F. Causone, Indoor environment data time-series reconstruction using autoencoder neural networks, Build. Environ. (2021) 191, https://doi.org/10.1016/j.buildenv.2021.107623.
[67] J. Kallio, J. Tervonen, P. Räsänen, R. Mäkynen, J. Koivusaari, J. Peltola, Forecasting office indoor CO2 concentration using machine learning with a one-year dataset, Build. Environ. (2021) 187, https://doi.org/10.1016/j.buildenv.2020.107409.
[68] S. Raghu, N. Sriraam, Optimal configuration of multilayer perceptron neural network classifier for recognition of intracranial epileptic seizures, Expert Syst. Appl. 89 (2017) 205–221, https://doi.org/10.1016/j.eswa.2017.07.029.
[69] W. Zhou, J. Jia, A learning framework for shape retrieval based on multilayer perceptrons, Pattern Recogn. Lett. (2018) 1–12, https://doi.org/10.1016/j.patrec.2018.09.005.
[70] R. Pino-Mejías, A. Pérez-Fargallo, C. Rubio-Bellido, J.A. Pulido-Arcas, Comparison of linear regression and artificial neural networks models to predict heating and cooling energy demand, energy consumption and CO2</Inf> emissions, Energy 118 (2017), https://doi.org/10.1016/j.energy.2016.12.022.
[71] R. Pino-Mejías, A. Pérez-Fargallo, C. Rubio-Bellido, J.A. Pulido-Arcas, Artificial neural networks and linear regression prediction models for social housing allocation: fuel poverty potential risk index, Energy 164 (2018) 627–641, https://doi.org/10.1016/j.energy.2018.09.056.
[72] A.R. Barron, Universal approximation bounds for superpositions of a sigmoidal function, IEEE Trans. Inf. Theor. 39 (1993) 930–945.
[73] G. Cybenko, Approximation by superpositions of a sigmoidal function, Math. Contr. Signals Syst. 2 (1989) 303–314.
[74] K. Hornik, M. Stinchcombe, H. White, Multilayer feedforward networks are universal approximators, Neural Network. 2 (1989) 359–366, https://doi.org/10.1016/0893-6080(89)90020-8.
[75] D.E. Rumelhart, G.E. Hinton, R.J. Williams, Learning representations by back-propagating errors, Nature 323 (1986) 533–536, https://doi.org/10.1038/323533a0.
[76] Y.N. Wang, A neural network adaptive control based on rapid learning method and application, Adv. Mold. Anal. 46 (1994) 27–34.
[77] P. Werbos, Beyond Regression: New Tools for Prediction and Analysis in the Behavior Science, Harvard University, 1974.
[78] R. Fletcher, Practical Methods of Optimization, John Wiley&Sons, Chichester - New York - Brisbane - Toronto, United States, 1980. ISBN 9780471277118.
[79] R.A. Kohavi, Study of cross-validation and bootstrap for accuracy estimation and model selection, in: Proceedings of the International Joint Conference on Artificial Intelligence, vol. 5, 1995.
[80] M. Sileo, F.T. Gizzi, A. Donvito, R. Lasaponara, F. Fiore, N. Masini, Multi-scale monitoring of rupestrian heritage: methodological approach and application to a case study, Int. J. Architect. Herit. (2020), https://doi.org/10.1080/15583058.2020.1799261.
[81] European Committee for Standardization, EN 15758 – Conservation of Cultural Property – Procedures and Instruments for Measuring Temperatures of the Air and the Surfaces of Objects, 2010.
[82] European Committee for Standardization, EN 16242 – Conservation of Cultural Heritage – Procedures and Instruments for Measuring Humidity in the Air and Moisture Exchanges between Air and Cultural Property, 2012.
[83] N. Nakicenovic, R. Swart, Special Report on Emissions Scenarios. A Special Report of Working Group III of the Intergovernmental Panel on Climate Change, Cambridge University Press, Cambridge, United Kingdom, 2000, ISBN 0-521-80493-0.
[84] American National Standards Institute/American Society of Heating Refrigerating and Air-Conditioning Engineers (ANSI/ASHRAE) ASHRAE, Guideline 14-2014: Measurement of Energy, Demand, and Water Savings, 2014.
[85] G.R. Ruiz, C.F. Bandera, Validation of calibrated energy models: common errors, Energies 10 (2017), https://doi.org/10.3390/en10101587.
[86] V. Ciancio, F. Salata, S. Falasca, G. Curci, I. Golasi, P. de Wilde, Energy demands of buildings in the framework of climate change: an investigation across Europe, Sustain. Cities Soc. (2020) 154244, https://doi.org/10.1016/j.scs.2020.102213.
[87] A. Roetzel, A. Tsangrassoulis, U. Dietrich, Impact of building design and occupancy on office comfort and energy performance in different climates, Build. Environ. 71 (2014) 165–175, https://doi.org/10.1016/j.buildenv.2013.10.001.
[88] M. Mourshed, The impact of the projected changes in temperature on heating and cooling requirements in buildings in Dhaka, Bangladesh, Appl. Energy 88 (2011) 3737–3746, https://doi.org/10.1016/j.apenergy.2011.05.024.
[89] A. Invidiata, E. Ghisi, Impact of climate change on heating and cooling energy demand in houses in Brazil, Energy Build. 130 (2016) 20–32, https://doi.org/10.1016/j.enbuild.2016.07.067.
[90] M.A. Triana, R. Lamberts, P. Sassi, Should we consider climate change for Brazilian social housing? Assessment of energy efficiency adaptation measures, Energy Build. 158 (2018) 1379–1392, https://doi.org/10.1016/j.enbuild.2017.11.003.
[91] H. Yassaghi, N. Mostafavi, S. Hoque, Evaluation of current and future hourly weather data intended for building designs: a philadelphia case study, Energy Build. 199 (2019) 491–511, https://doi.org/10.1016/j.enbuild.2019.07.016.
[92] D. Bienvenido-Huertas, C. Rubio-Bellido, J.A. Pulido-Arcas, A. Pérez-Fargallo, Towards the implementation of periodic thermal transmittance in Spanish building energy regulation, Journal of Building Engineering 31 (2020), https://doi.org/10.1016/j.jobe.2020.101402.
[93] G.R. Roshan, R. Oji, S. Attia, Projecting the impact of climate change on design recommendations for residential buildings in Iran, Build. Environ. 155 (2019) 283–297, https://doi.org/10.1016/j.buildenv.2019.03.053.
[94] S. Attia, P. Eleftheriou, F. Xeni, R. Morlot, C. Ménézo, V. Kostopoulos, M. Betsi, I. Kalaitzoglou, L. Pagliano, M. Cellura, et al., Overview and future challenges of nearly zero energy buildings (NZEB) design in southern Europe, Energy Build. 155 (2017) 439–458, https://doi.org/10.1016/j.enbuild.2017.09.043.